Hu, Junjie; Kuo, Weiyu; Härdle, Wolfgang Karl

Working Paper

Risk of Bitcoin Market: Volatility, Jumps, and Forecasts

IRTG 1792 Discussion Paper, No. 2019-024

Provided in Cooperation with:
Humboldt University Berlin, International Research Training Group 1792 "High Dimensional Nonstationary Time Series"

Suggested Citation: Hu, Junjie; Kuo, Weiyu; Härdle, Wolfgang Karl (2019) : Risk of Bitcoin Market: Volatility, Jumps, and Forecasts, IRTG 1792 Discussion Paper, No. 2019-024, Humboldt-Universität zu Berlin, International Research Training Group 1792 "High Dimensional Nonstationary Time Series", Berlin

This Version is available at:
https://hdl.handle.net/10419/230800

IRTG 1792 Discussion Paper 2019-024

Risk of Bitcoin Market: Volatility, Jumps, and Forecasts

Junjie Hu [*]
Weiyu Kuo [*2]
Wolfgang Karl Härdle [* *3 *4 *5]

[*] Humboldt-Universität zu Berlin, Germany
[*2] National Chengchi University, Taiwan
[*3] Singapore Management University, Singapore
[*4] Xiamen University, China
[*5] Charles University Prague, Czech Republic

This research was supported by the Deutsche Forschungsgesellschaft through the International Research Training Group 1792 "High Dimensional Nonstationary Time Series".

http://irtg1792.hu-berlin.de
ISSN 2568-5619

Risk of Bitcoin Market: Volatility, Jumps, and Forecasts *

Junjie Hu†, Weiyu Kuo‡, Wolfgang Karl Härdle§

01.10.2019

Abstract

Among all the emerging markets, the cryptocurrency market is considered the most controversial and simultaneously the most interesting one. The visibly significant market capitalization of cryptos motivates modern financial instruments such as futures and options. Those will depend on the dynamics, volatility, or even the jumps of cryptos. In this paper, the risk characteristics for Bitcoin are analyzed from a realized volatility dynamics view. The realized variance RV is estimated with (threshold-)jump components $(T)J$, semivariance $RSV^{+(-)}$, and signed jumps $(T)J^{+(-)}$. Our empirical results show that the Bitcoin market is far riskier than any other developed financial market. Up to 68% of the sample days are identified to entangle jumps. However, the discontinuities do not contribute to the variance significantly. By employing a 90-day rolling-window method, the in-sample evidence suggests that the impacts of predictors change over time systematically under HAR-type models. The out-of-sample forecasting results reveal that the forecasting horizon plays an important role in choosing forecasting models. For long-horizon risk forecast, a finer model calibrated with jumps gives extra utility up to 20 basis points annually, while an approach based on the roughest estimators suits the short-horizon risk forecast best. Last but not least, a simple equal-weighted portfolio not only significantly reduces the size and quantity of jumps but also gives investors higher utility in short-horizon risk forecast case.

JEL classification: C53, E47, G11, G17,

Keywords: Cryptocurrency, Bitcoin, Realized Variance, Thresholded Jump, Signed Jumps, Realized Utility

* Supported by Deutsche Forschungsgemeinschaft via IRTG 1792 "High Dimensional Nonstationary Time Series", Humboldt-Universität zu Berlin. All supplementary and Python code can be obtained: QRCVJ_Forecasting

† Corresponding author. Humboldt-Universität zu Berlin. Spandauer Str. 1, 10178 Berlin, Germany. Email: hujunjie@hu-berlin.de

‡ Department of International Business and Risk and Insurance Research Center, National Chengchi University, Taipei City, Taiwan 116. Email: wkuo@nccu.edu.tw

§ C.A.S.E. - Center for Applied Statistics and Economics, Humboldt-Universität zu Berlin; Sim Kee Boon Institute for Financial Economics, Singapore Management University; Wang Yanan Institute for Studies in Economics, Xiamen University; Department of Mathematics and Physics, Charles University Prague. Email: haerdle@hu-berlin.de

1. Introduction

Understanding and managing risk of Bitcoin, an emerging cryptocurrency, is crucial for financial investment and construction of contingent claims. Typically, risk is decomposed into variance and jumps. The variance describes the intensity of price changing, while the jumps indicate discontinuities points of price. Different assets may have similar risk characteristics, however, for the Bitcoin market, it can be viewed to be one of the outliers in the sense of increased volatility and more frequent jumps.

The inherent risk of Bitcoin (BTC) comes from its unregulated technologic nature. Different from fiat currencies issued and endorsed by governments, BTC is an unprecedented "currency" that thrives without being supervised or regulated. BTC was first proposed by Nakamoto (2008) and then initialized in 2009. For the first few years after being created, it was unknown to most people but some of the technology enthusiasts. It is built on the blockchain technology which decentralizes and distributes information through networks worldwide. This decentralized system is controlled by an algorithm that adds new blocks on the blockchain-based on consensus from the whole network. BTC is essentially a derivative or incentive that the algorithm rewards the person who spends computation power and wins the authority to write a new block. Hence, BTC is a naturally decentralized currency as being part of blockchain. Nevertheless, regulations can be enforced to the exchanges in which BTC and any other cryptocurrencies are traded. We conduct this research by using the data from some of the regulated exchanges.

A series of literature discusses the function of cryptocurrencies. On one hand, Yermack (2015) argues that BTC is rather a speculative investment than a "currency" because of reasons such as its price is too volatile for users, low acceptance from common merchants, etc. Some articles find evidence that BTC has strong speculative bubble properties by using bubble testing methods, such as Hafner (2018) and Gerlach, Demos, and Sornette (2019). Griffin and Shams (2018) document possible price manipulations. Due to lack to fundamental value, papers find that the latent drivers of BTC price and volatility could be the sentiment, a series of social signals such as opinions and trading volume (Bukovina, Martiček, et al. (2016); Garcia and Schweitzer (2015); Balcilar, Bouri, Gupta, and Roubaud (2017)). On the other hand, BTC is considered from the aspect of portfolio management. BTC is found to function as a hedging or risk haven asset (Bouri, Molnár, Azzi, Roubaud, and Hagfors (2017); Urquhart and Zhang (2019)) and it has similar properties like gold under the assymmetric GARCH models (Gronwald (2014); Dyhrberg (2016)). Glaser, Zimmermann, Haferkorn, Weber, and Siering (2014) argue that people use BTC not for transactions but as an alternative investment. Other than the discussions on the economic role of BTC,

researchers also study BTC from the econometrics angle, starting from the construction of cryptocurrencies index (Trimborn and Härdle (2018)) and preliminary econometric modelling (Chen, Chen, Härdle, Lee, and Ong (2018)). A recent paper of Traian Pele, Niels, Härdle, Kolossiatis, and Yatracos (2019) classify cryptocurrency as a new asset class by its statistical feature.

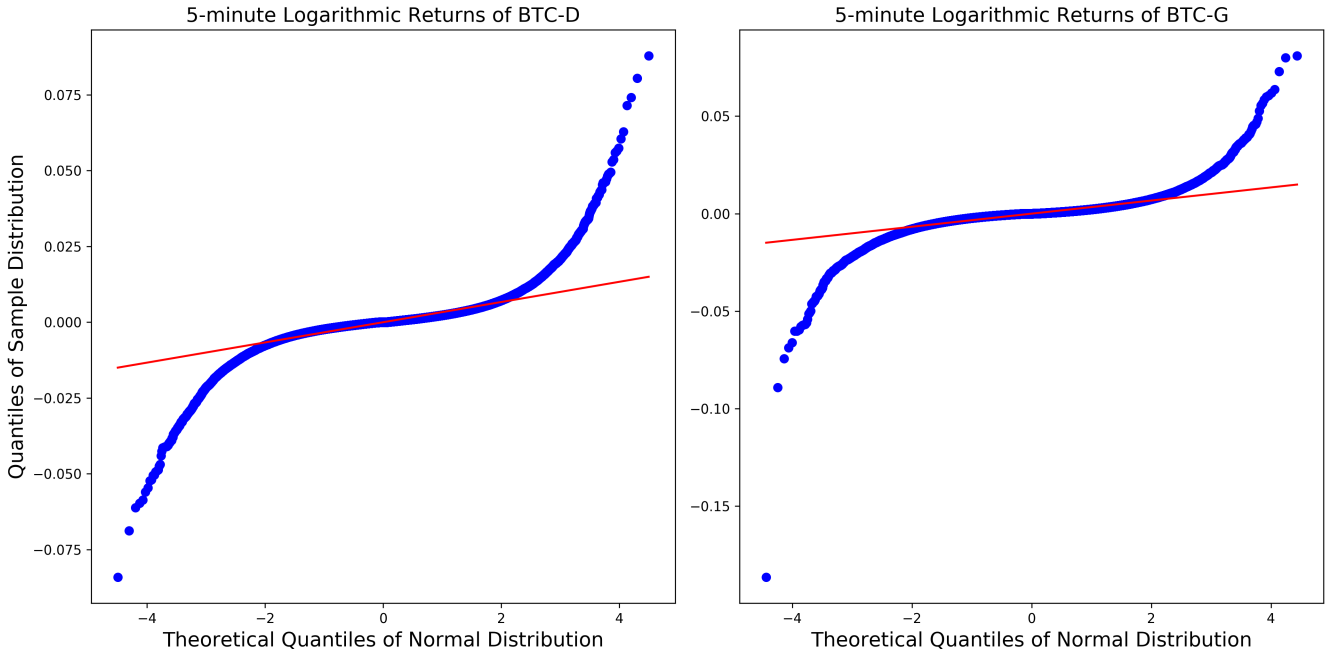

Figure 1: Q-Q plot on 5-minute logarithmic returns of BTC-D (left panel) and BTC-G (right panel). Any of the observations has trading volume located below 50% quantile is filtered out. Sample period starts from January 2017 to May 2019

QRiskBTC_Plot

BTC has frequently experienced extreme variance and jumps on price since 2013. The Bitcoin market started to draw attention in 2013 when the unit price exceeded 100 U.S. dollars. 4 years later, in January 2017, the unit price hit 1000 U.S. dollars and reached almost 20,000 U.S. dollars by the end of 2017. The bubble burst in 2018, its price dropped around 80% from the peak in one year and it is again climbing up in 2019. The high volatility entangled with jumps phenomenon of the Bitcoin market is evidenced by the Q-Q plot on 5-minute logarithmic returns shown in Figure 1. One can observe the fat-tail effect on BTC logarithmic return distribution.

Apart from many of the online exchanges offering BTC futures and options, the strictly regulated exchange CME launched futures on BTC in 2017. More and more investors/speculators enter the cryptocurrency markets and its derivatives markets demanding studies on BTC risk from an academic point of view. Conrad, Custovic, and Ghysels (2018) decomposes the volatility into short term and long term components by GARCH-MIDAS analysis, and

study the volatility correlation between BTC and some other indices, for example, Baltic dry index. Other papers focus on the forecasting side, for example, Pichl and Kaizoji (2017). One recent paper of Scaillet, Treccani, and Trevisan (2018) analyze the jump behavior using the dataset from Mt. Gox exchange on the sample period from 2011 to 2013. And papers, for example, Hou, Wang, Chen, and Härdle (2018) attempt to calibrate an option pricing model adapting the high volatility and jump properties.

Table 1: Summary Statistics of BTC Annualized Realized Variance Against Global Exchange Indices

	AEX†	DJI†	FTSE†	HSI†	SPX†	SSEC†	BTC-D	BTC-G
count	4 842	4 704	4 769	4 645	4 709	4 508	864	883
mean	0.16	0.12	0.14	0.15	0.13	0.23	1.16	0.93
std	0.38	0.30	0.32	0.41	0.32	0.46	2.05	1.76
min	0.10%	0.08%	0.16%	0.35%	0.04%	0.23%	0.02	0.76%
25%	0.02	0.02	0.02	0.03	0.02	0.03	0.08	0.04
50%	0.05	0.04	0.05	0.06	0.05	0.09	0.56	0.40
75%	0.14	0.11	0.13	0.14	0.12	0.23	3.70	3.17
max	7.04	5.55	7.74	16.46	7.18	7.71	26.07	21.99

†: Selected global indices from developed markets and emerging markets. Trading hours in different global exchanges could be different which introduce bias of RV. We correct such bias by accounting the overnight price change (Bollerslev, Hood, Huss, and Pedersen (2018)) to allow those RV estimators to be comparable.
Datasource from Realized Library, Oxford-Man Institute of Quantitative Finance.

Volatility plays a key role in observing market uncertainty and modeling dynamics of financial assets. As the second moment of a random process, it is also the core element of pricing financial derivatives, optimizing portfolios and risk management(Fleming, Kirby, and Ostdiek (2001)). The Realized Variance RV which accounts intraday information from high-frequency data, essentially the sum of squared returns over the period, was advocated by previous literature (see e.g Andersen, Bollerslev, Diebold, and Labys (2001); Barndorff-Nielsen and Shephard (2002a)). Andersen, Bollerslev, Diebold, and Ebens (2001) document that this model-free estimate is highly right-skewed, logarithmic normal distributed and characterized by a strong temporal dependency property.

We start with constructing RV by using the 5-minute high-frequency BTC price data from two data sources named BTC-D and BTC-G. Due to Bitcoin market liquidity constraint before 2017, we fix the sample period from January 2017 until May and July 2019. The extraordinary higher risk level of BTC stands out immediately comparing with any other developed financial markets, as shown in Tab.1.

In practice, a continuous diffusion sample path assumption rarely holds and discontinuity should be accounted in. We separate jump components J based on model provided by Barndorff-Nielsen and Shephard (2004). However, this estimator is biased for BTC which suffers from consecutive jumps. Hence the Thresholded Jump TJ estimator from Corsi,

Pirino, and Reno (2010) is employed. TJ detects more jumps than J does, and both estimators indicate that jumps happened in Bitcoin market much more frequently compared with results on other traditional assets. Surprisingly, despite the large size and quantity of jumps detected in BTC, the discontinuities do not contribute much to risk. Further, we decompose RV into upside/downside variance $RSV^{+(-)}$ (Barndorff-Nielsen, Kinnebrock, and Shephard (2008)) and yield the positive/negative jump components $(T)J^{+(-)}$. Contrary to the result from Scaillet, Treccani, and Trevisan (2018), we find approximately the same number of positive and negative jumps. This finding may be attributed to the longer sample period.

We develop 8 forecasting models accounting different jump estimators which are motivated by Heterogeneous AutoRegression (HAR) model introduced in Corsi (2009). First, the full-sample fitting gives inconsistent results estimating the average effect of each estimators impacting on RV. Then we allow the parameters changing over time by employing a 90-day rolling window forecasting method. The performance of forecasting models heavily rely on forecasting horizon, i.e the finer calibrated models outperform in the long horizon forecast while the roughest model HAR performs best in the short-horizon forecast. Such a finding is further confirmed by a utility-based framework (Bollerslev, Hood, Huss, and Pedersen (2018)). A finer model outperforms HAR up to 20 basis points for in the 30-day horizon forecast but underperforms in the 1-day horizon forecast. Last but not least, the simple equal-weighted portfolio BTC-D not only reduces the idiosyncratic jump risk significantly but also provides extra utility in the short-horizon risk forecasting case.

We will proceed with the article as follows. In section 2, we briefly describe theoretical models used in this article including realized variance, jumps, thresholded jumps, realized semivariance, and signed jumps. Then, in section 3, we present the data we use, followed by a discussion on BTC price processes and the liquidity of BTC Market, and summary statistics on realized variance and jumps. Section 4 discuss the construction and comparison of forecasting models and the forecasts are evaluated under a utility-based framework. Finally, we conclude our findings and remarks in section 5.

2. Theoretical Framework

Realized variance and jumps have been developed in the recent two decades. In this section, we present the construction of the estimators used in this article. Starting with the Realized Variance RV, we introduce the Jump component J separated from RV by the BiPower Variance BPV. To overcome the bias caused by consecutive jumps, the corrected Thresholded BiPower Variance $TBPV$ is used to separate it from Thresholded Jump TJ. Furthermore, in order to decompose the jump component into positive and negative $J^{+(-)}$,

we employ the Realized SemiVariance $RSV^{+(-)}$.

All estimators are constricted in a continuous-time jump diffusion process framework, i.e for a logarithmic asset price $p(t)$:

$$\mathrm{d}\, p(t) = \mu(t)\,\mathrm{d}\, t + \sigma(t)\,\mathrm{d}\, W(t) + \kappa(t)\,\mathrm{d}\, q(t), 0 \leq t \leq T \tag{1}$$

where $\mu(t)$ is a continuous process with bounded local variation, $\sigma(t)$ is a càdlàg process, $W(t)$ is Brownian motion. The third term on the right-hand side is the jump process, where q counts the number of jumps with time-varying intensity denoted by κ.

This article uses logarithmic returns $r_{t+j\Delta} \stackrel{\text{def}}{=} p\,(t + j\Delta) - p\,(t + (j-1)\Delta)$ which denotes the *j-th* observed value in day t, the given sampling step Δ will be introduced latter.

2.1. Realized Variance and Jumps

Realized variance $RV_{t,t+1}$ is simply the cumulative squared logarithmic returns over time period $[t, t+1]$: (For convenience, we omit one t, i.e $RV_{t+1} = RV_{t,t+1}$)

$$RV_{t+1}(\Delta) \stackrel{\text{def}}{=} \sum_{j=1}^{1/\Delta} r_{t+j\Delta}^2 \tag{2}$$

To calculate 2, $[t, t+1]$ is partitioned into N intervals evenly. The sampling step is $\Delta = 1/N$, for example, with 288 observations each day, $\Delta = 1/288$. By the theory of quadratic variation, the increment of Quadratic Variation QV of $p(t)$ can be expressed as:

$$\begin{aligned} QV_{t+1} &= \operatorname*{p\text{-}lim}_{\Delta \to 0} \sum_{j=1}^{1/\Delta} r_{t+j\Delta}^2 \\ &= \int_t^{t+1} \sigma^2(s) ds + \sum_{t<s\leq t+1} \kappa^2(s) \end{aligned} \tag{3}$$

The variation of $p(t)$ measured by QV comes from two sources, one is driven by the càdlàg process and one is caused by the jump process. A series of literature discuss the convergence properties of RV. Andersen, Bollerslev, Diebold, and Labys (2001), Barndorff-Nielsen and Shephard (2002a), Barndorff-Nielsen and Shephard (2002b) document the absence of jumps. Later, Barndorff-Nielsen and Shephard (2004), Barndorff-Nielsen and Shephard (2006), Andersen, Bollerslev, and Diebold (2007) generalize to possible jumps. RV converges in probability to QV as Δ goes to 0:

$$RV_{t+1}(\Delta) \xrightarrow{\text{p}} \underbrace{\int_t^{t+1} \sigma^2(s)ds}_{IV_{t+1}} + \underbrace{\sum_{t<s\leq t+1} \kappa^2(s)}_{J_{t+1}} \tag{4}$$

Hence, RV consists of two components: The continuous IV component, and the Jump component J. The BiPower Variation BPV measuring the continuous process allows to separate the components

$$BPV_{t+1}(\Delta) = \mu_1^{-2} \sum_{j=2}^{1/\Delta} |r_{t+j\Delta}| \cdot |r_{t+(j-1)\Delta}|, \tag{5}$$

where $\mu_1 = \sqrt{2/\pi}$. BPV converges in probability to IV in (4) as Δ goes to 0. A general form of BPV is the MultiPower Variance, see Appendix A.1.

Intuitively, BPV is robust to an infrequent jump process as the variation process is smoothed by cumulating the adjacent logarithmic returns. J can therefore be isolated by taking the difference of RV and BPV. And then the difference is truncated to guarantee that J is non-negative, see 6.

$$\begin{aligned} BPV_{t+1}(\Delta) &\xrightarrow{\text{p}} \int_t^{t+1} \sigma^2(s)ds \\ RV_{t+1}(\Delta) - BPV_{t+1}(\Delta) &\xrightarrow{\text{p}} \sum_{t<s\leq t+1} \kappa^2(s) \\ J_{t+1} &\stackrel{\text{def}}{=} \max\left\{RV_{t+1}(\Delta) - BPV_{t+1}(\Delta), 0\right\} \end{aligned} \tag{6}$$

2.2. Threshold Bipower Variance and Jumps

BPV is effective in the sense of smoothing a variation process when both size and quantity in the jump process are relatively small, in other words, BPV is biased to large and consecutive jumps which are not evidently appropriated for investigating cryptocurrencies. For example, Fig.2 shows that consecutive jumps occurred in case the variation process is not smoothed by BPV. Empirical evidence shown in Fig.3 indicates that the $BPV^{1/2}$ process is very similar to the $RV^{1/2}$ process which in turn cause the $J^{1/2}$ estimator biased.

To alleviate such bias, we implement the threshold variation model of Corsi, Pirino, and Reno (2010). The main idea of Thresholded MultiPower Variation $TMPV$ is documented in Mancini (2009) which essentially truncates any logarithmic return when it exceeds a certain level θ, see more details in Appendix A.2.

At time point $t + j\Delta$, the threshold value $\theta_{t+j\Delta}$ is varying along with local variance $\widehat{V}_{t+j\Delta}$

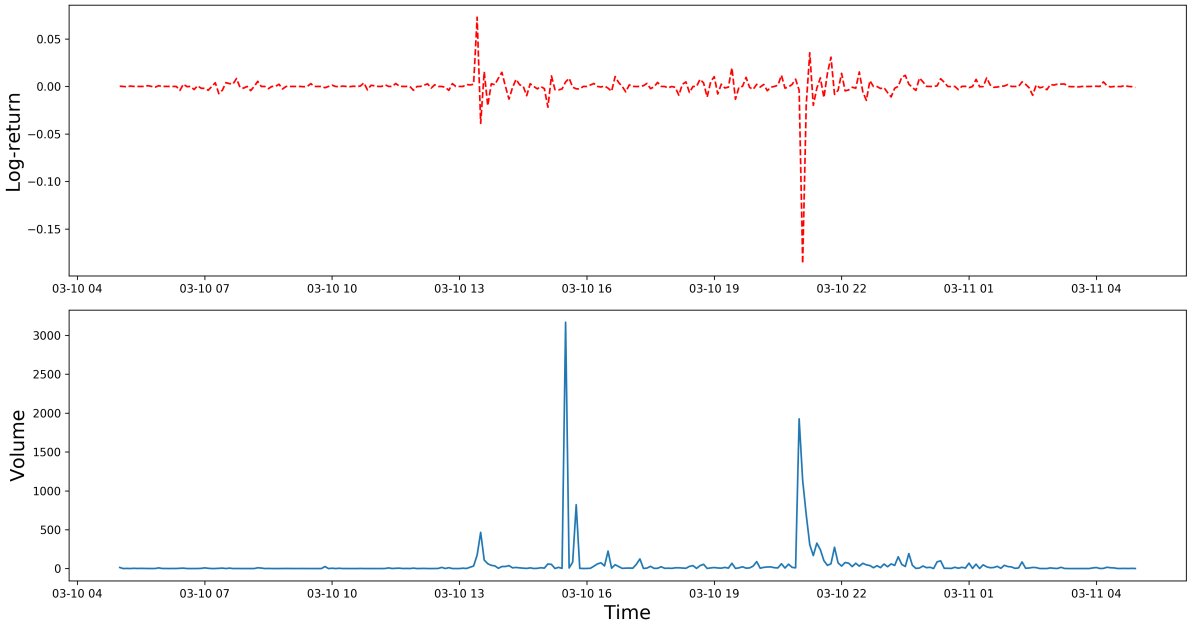

FIGURE 2: A trajectory of the intraday behavior of BTC-G, 10th Mar. 2017. Upper panel shows the logarithmic return process and the bottom panel is the corresponding trading volume. Both in 5-minute sampling frequency.

for given constant coefficient, i.e $\theta_{t+j\Delta} = c_\theta^2 \cdot \widehat{V}_{t+j\Delta}$

Corsi, Pirino, and Reno (2010) shows that any unbiased estimator for realized local variance σ^2 can be implemented, e.g the Fan and Yao (2008) estimator we use detailed in Appendix A.3 which is essentially a kernel smoothing estimator.

Given the local variation estimate $\widehat{V}_{t+j\Delta}$, the constant c_θ also impacts $TMPV$. As c_θ goes larger $TMPV$ truncates less values, hence $TMPV$ goes to MPV. In our main empirical results, we follow the literature and choose $c_\theta = 3$.

Given the estimation of threshold value $\theta_{t+j\Delta}$, Mancini and Renò (2011) proposes the way of directly truncating the returns exceeded the threshold. However, this could also annihilate some of the price changes for $TBPV$ that are not "real" jumps which in turn cause more "fake" jumps been detected. Hence, we implement the corrected version of $TMPV$ that relieve such "double-sword" bias (Corsi, Pirino, and Reno (2010)). To avoid confusion, $TMPV$ is short for the corrected version of $TMPV$ hereafter.

Essentially, instead of eliminating every of the points that has square-returns $r^2_{t+j\Delta}$ larger than certain threshold value $\theta_{t+j\Delta}$, the corrected $TMPV$ replaces the η-th power logarithmic return $|r|^\eta_{t+j\Delta}$ with $r^e(\theta_{t+j\Delta}, \eta)$ which is the expected value under assumption that $r_{t+j\Delta} \sim N(0, \sigma^2)$. The conditional replacement logarithmic return $C_\eta(r_{t+j\Delta}, \theta)$ can be written as:

(A) Jump of **BTC-D** separated from **BPV**. From 1st January 2017 to 31st May 2019

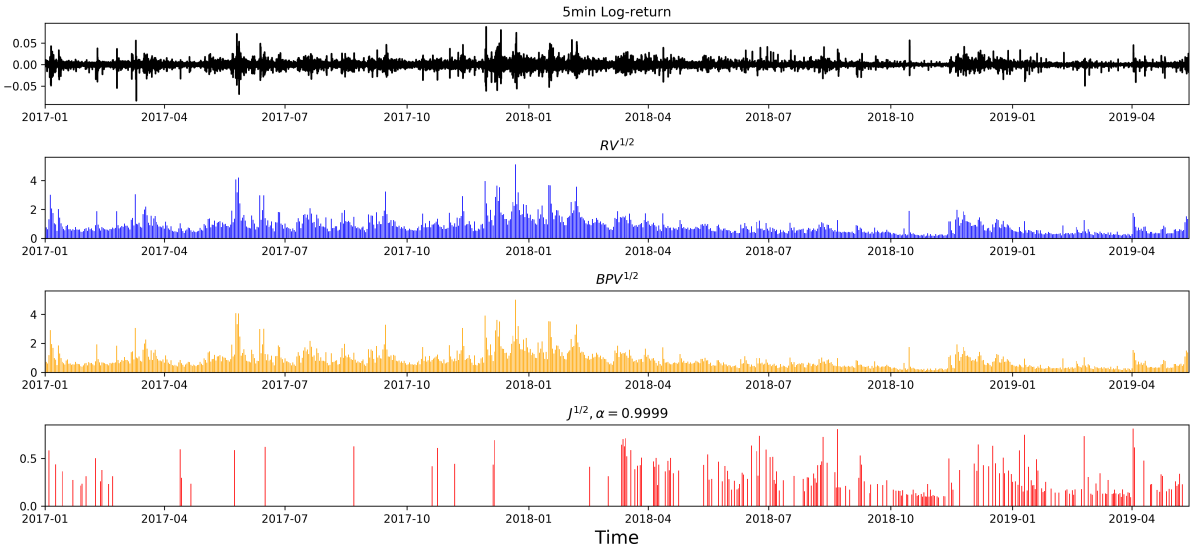

(B) Jump of **BTC-G** separated from **BPV**. From 1st January 2017 to 31st July 2019

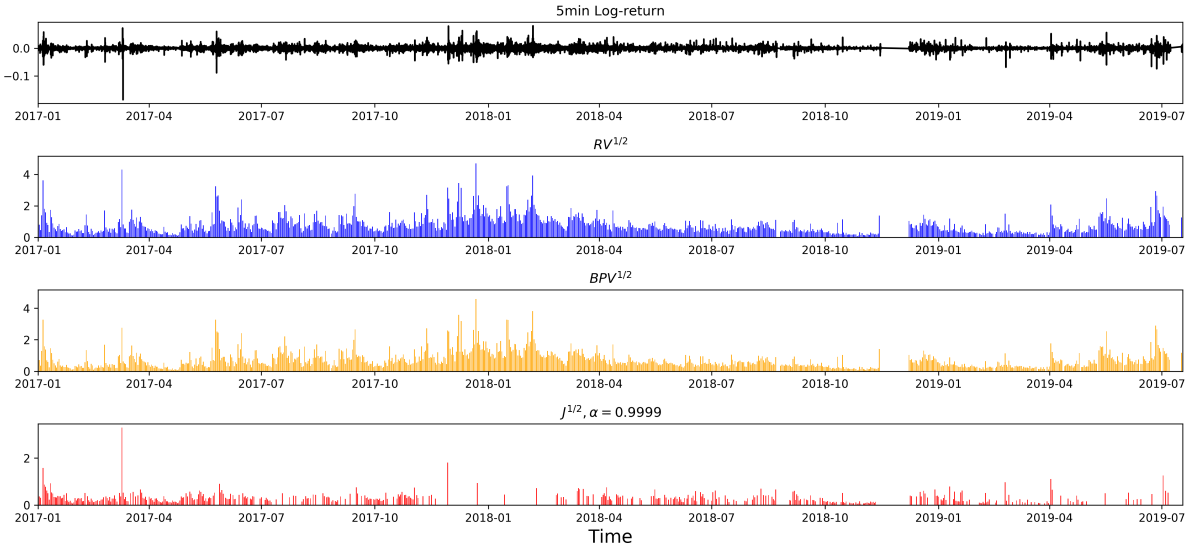

FIGURE 3: Jump Separation by BPV estimator. The panels from top to bottom are the 5-minute logarithmic returns, realized volatility ($RV^{1/2}$), bipower volatility ($BPV^{1/2}$) and separated significant jump in square root form ($J^{1/2}$) under confidence level $\alpha = 99.99\%$. Test for significant J is detailed in AppendixA.6

$$C_\eta(r_{t+j\Delta}, \theta_{t+j\Delta}) = \begin{cases} |r_{t+j\Delta}|^\eta & , r^2_{t+j\Delta} \leq \theta \\ r^e_{t+j\Delta}(\theta_{t+j\Delta}, \eta) & , r^2_{t+j\Delta} > \theta \end{cases} \tag{7}$$

More details about expected logarithmic return $r^e_t(\theta_t, \eta)$ is documented in Appendix A.4.

Similar to procedure for detecting J, two special cases of $TMPV$ are used here. $TBPV$ estimates $\int_t^{t+1} \sigma^2(s)ds$ and $TTPV$ estimates $\int_t^{t+1} \sigma^4(s)ds$. Two estimators are defined as follows. The general form of corrected $TMPV$ is detailed in the Appendix A.5.

$$TBPV_{t+1}(\Delta) = \mu_1^{-2} \cdot \sum_{j=2}^{1/\Delta} C_1(r_{t+j\Delta}, \theta_{t+j\Delta}) C_1(r_{t+(j-1)\Delta}, \theta_{t+(j-1)\Delta}) \tag{8}$$

$$\begin{aligned} TTPV_{t+1}(\Delta) = \mu_{\frac{4}{3}}^{-3} \cdot \Delta^{-1} \cdot \sum_{j=3}^{1/\Delta} & C_{\frac{4}{3}}\left(r_{t+j\Delta}, \theta_{t+j\Delta}\right) \\ & \cdot C_{\frac{4}{3}}\left(r_{t+(j-1)\Delta}, \theta_{t+(j-1)\Delta}\right) \\ & \cdot C_{\frac{4}{3}}\left(r_{t+(j-2)\Delta}, \theta_{t+(j-2)\Delta}\right) \end{aligned} \tag{9}$$

Test for thresholded jumps t-z is given by (10), provided by Corsi, Pirino, and Reno (2010) which is based on the ratio statistic from Huang and Tauchen (2005), detailed by Andersen, Bollerslev, and Diebold (2007)(z, see Appendix A.6) under continuous jump diffusion model. Where $\zeta = \frac{\pi^2}{4} + \pi - 5$. Under a series assumptions, for the null hypothesis that no jump exists, t-z converges to standard normal distribution as Δ goes to 0, i.e t-$z \xrightarrow{\mathcal{L}} N(0,1)$.

$$t\text{-}z_{t+1} = \frac{\left\{RV_{t+1}(\Delta) - TBPV_{t+1}(\Delta)\right\} RV_{t+1}^{-1}(\Delta)}{\sqrt{\Delta \cdot \zeta \cdot \max\left\{1, \frac{TTPV_{t+1}(\Delta)}{\{TBPV_{t+1}(\Delta)\}^2}\right\}}} \tag{10}$$

Then, we can calculate the Threshold realized Jumps TJ, taking account only the significant jumps by t-z test. Likewise, we also use the z test to retain only the significant jumps J in (6)

$$TJ_{t+1}(\Delta) = \max\left\{RV_{t+1}(\Delta) - TBPV_{t+1}(\Delta), 0\right\} \cdot \mathbf{I}\left\{t\text{-}z_{t+1} > \Phi_\alpha\right\} \tag{11}$$

Consequently, we can enforce the $RV = (T)C + (T)J$, thus the continuous component $(T)C_{t+1}(\Delta) = RV_{t+1}(\Delta) - (T)J_{t+1}(\Delta)$.

By the comparison between Fig.(4) with Fig.(3), under confidence level $\alpha = 99.99\%$, the threshold method $TBPV$ detects more significant jumps than BPV method. We will further discuss the dynamics of those two estimators and compare the performance under forecasting models.

2.3. Realized Semivariance and Signed Jumps

In the subsection, we go further to discuss the detection of positive and negative jumps. Recall that under the continuous jump diffusion model assumption, the jump component of quadratic variation QV_{t+1} is the accumulated sum of squared infinitesimal changes $\Delta p_s = p_s - p_{s_-}$, i.e $\sum_{t<s\leq t+1}(\Delta p)^2(s)$. Hence, the jump component is guaranteed to be non-negative

(A) BTC-D Jump separation from 1st January 2017 to 31st May 2019

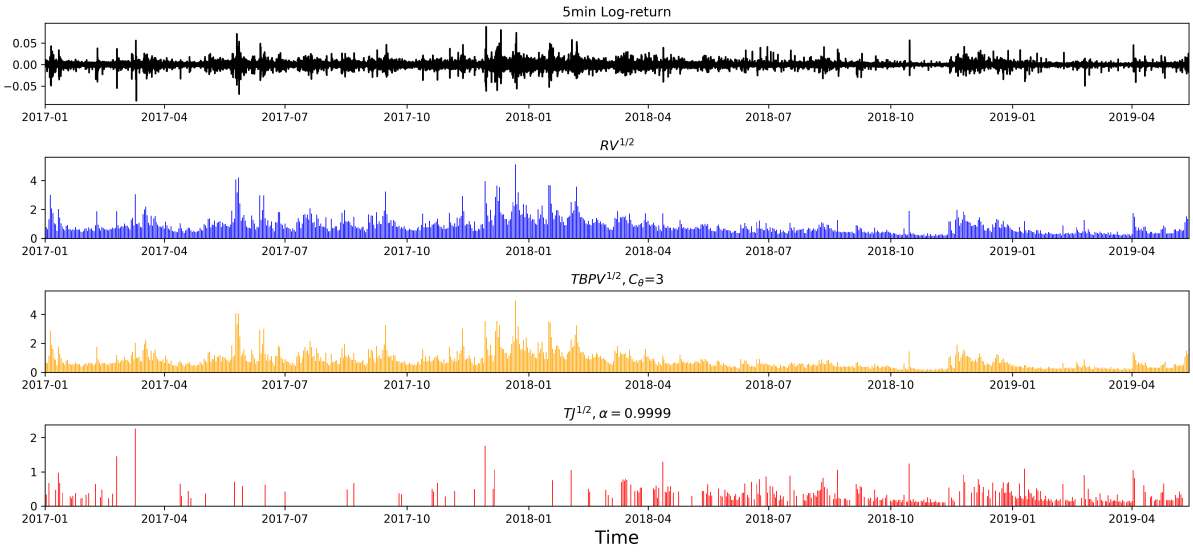

(B) BTC-G Jump separation from 1st January 2017 to 31st July 2019

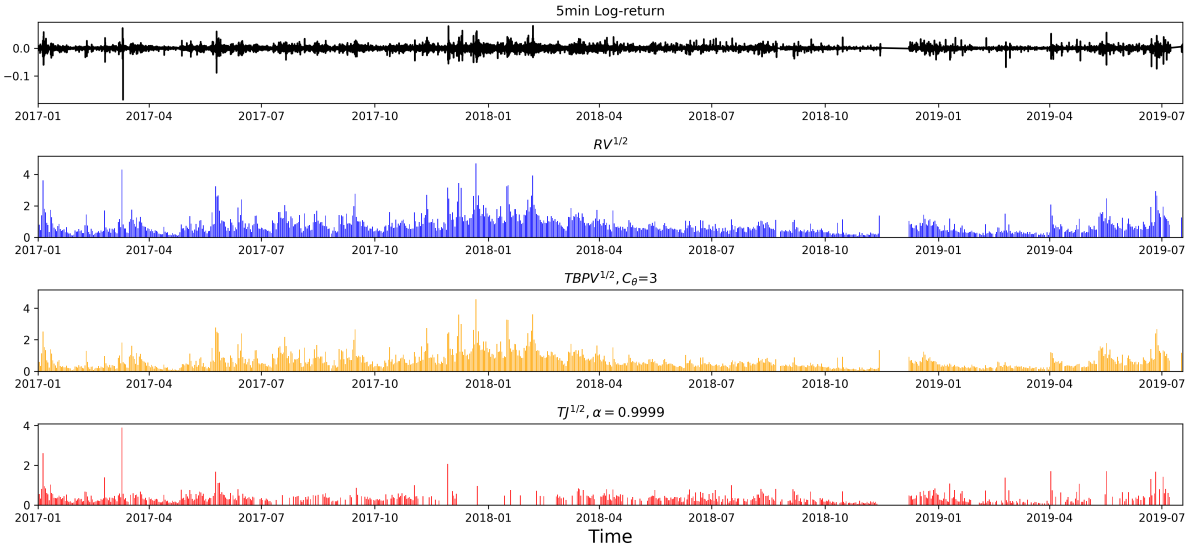

FIGURE 4: The panels from top to bottom are logarithmic return, square-root form of realized volatility ($RV^{1/2}$), square-root form of threshold bipower variance ($TBPV^{1/2}$) with $c_\theta = 3$ and separated significant jump process in square-root form ($TJ^{1/2}$) under confidence level $\alpha = 99.99\%$

as defined in (11). On the other hand, from the finance perspective, investors are keen to understand the dynamics of the positive and negative jump, especially how those estimators impact the market of their interests. For example, the asymmetric effect of positive and negative risk on asset returns are well investigated in previous literature.

Realized semivariance RSV (Barndorff-Nielsen, Kinnebrock, and Shephard (2008)) provides us one way to separate positive and negative jumps from the realized variance process. The definition of positive (negative) $RSV^{+(-)}$ shown in (12) is essentially the the sum of the

squared positive (negative) logarithmic returns.

$$RSV_{t+1}^{+(-)} = \sum_{j=1}^{1/\Delta} r_{t+j\Delta}^2 \cdot \mathbf{I}\{r_{t_j\Delta} > (<)0\} \tag{12}$$

It is straight forward that RV can be decomposed into RSV^+ and RSV^- completely, i.e $RV = RSV^+ + RSV^-$, for both finite sample and large sample cases. As sampling frequency $1/\Delta$ goes infinite, the limiting behavior of RSV given by (13) under infill asymptotics shows that $RSV^{+(-)}$ converges to one-half of the integrated variance and positive (negative) sum of squared jumps. Such decomposition is also evidenced by our empirical result that the sum of the average value of RSV^+ and RSV^- is almost the average value of RV.

$$RSV_{t+1}^{+} \xrightarrow{p} \underbrace{\frac{1}{2}\int_t^{t+1} \sigma^2(s)ds}_{\frac{1}{2}IV_{t+1}} + \underbrace{\sum_{t<s\leq t+1} (\Delta p_s)^2 \cdot \mathbf{I}\{\Delta p_s > 0\}}_{J_{t+1}^+} \tag{13}$$

With this convergence property above and the property of BPV described in (6), one can easily separate the (Thresholded) Positive Jumps $(T)J^+$ or (Thresholded) Negative Jumps $(T)J^-$ by subtracting RSV^+ or RSV^- by $(T)BPV$. As defined in (14), we will have four signed jump estimators, J^+, J^-, TJ^+, TJ^-.

$$(T)J_{t+1}^{+(-)} = \max\left\{RSV_{t+1}^{+(-)} - \frac{1}{2}(T)BPV_{t+1}, 0\right\} \tag{14}$$

3. Data and Preliminary Analysis

We construct two price processes from two data sources to highlight the robustness of our empirical results on the risk of Bitcoin which is traded among many online exchanges. This section can be roughly divided into 3 parts. We start with introducing our dataset, followed by the discussion on the characteristics of the two price processes and liquidity of Bitcoin market. Finally, we present the summary statistics of realized variance and jump components.

3.1. Data Source

There are 254[1] online exchanges trading various types of cryptocurrencies and each of them is traded in different exchanges globally. Among all crypto markets, Bitcoin market is dominant with more than 70% market share. We focus only on Bitcoin market, two price

[1]Until July 2019, https://coin.market/exchanges-info.php

processes constructed from two different data sources are studied. One process is from a private data source called DYOS[2], hereafter **BTC-D**, and the other one is an online free provider [3], hereafter **BTC-G**. BTC-D price is equal-weighted prices from three actively trading exchanges, Poloniex, Bittrex, and Bitfinex[4]. Such construction can be viewed as a portfolio-type price which allows investors to avoid idiosyncratic risk from exchanges. And BTC-G price comes from only one exchange, Gemini[5], which is one of the largest digital exchanges regulated by NYDFS[6].

The full dataset can be dated back to 2014, however, the trading was inactive and prices were not efficient until 2017, thus we truncate both datasets and start them from January 2017. The BTC-D process lasts until May 2019, and BTC-G process goes to July 2019. After cleaning and removing the trading days that have the incomplete number of samples, the dataset has totally 864-day samples for BTC-D and 883-day samples for BTC-G. Both two data sources are sampled every 5-min, thus every day has 288 samples.

3.2. Price Process of BTC

A series of literature have discussed sampling frequency issues regarding realized variance estimator impaired by microstructure noise, e.g Ait-Sahalia, Mykland, and Zhang (2005) and Bandi and Russell (2008) attempt to derive optimal sampling frequency by explicitly assuming noise structure, Zhang, Mykland, and Aït-Sahalia (2005) Zhang (2006) document the efficient estimator by subsampling schemes, and kernel methods are introduced to handle the noise (Barndorff-Nielsen, Hansen, Lunde, and Shephard (2008); Hansen and Lunde (2006)). Liu, Patton, and Sheppard (2015) tests estimators constructed with different sampling frequency and finds no evidence against 5-minute sampling strategy. For simplicity, following most of the empirical literature such as Andersen, Bollerslev, Diebold, and Ebens (2001); Andersen, Bollerslev, and Diebold (2007), this paper employs the 5-minute high-frequency sampling strategy for both BTC-D and BTC-G, i.e taking the close price of each 5-minute interval.

Like fiat currencies, the price of BTC is essentially an exchange rate against another currency. In most of the exchanges, there are two notions of BTC price. BTC price can be denoted by either U.S dollars or another cryptocurrency named USDT.

Here we have some introduction of USDT regarding its reliability. The USDT is an innovative cryptocurrency that claims to tether U.S. dollar with a 1:1 exchange rate. Such

[2]Dyos solutions GmbH, Berlin, Germany
[3]https://www.cryptodatadownload.com/
[4]Poloniex and Bittrex are U.S based companies, and Bitfinex located in Hongkong
[5]https://gemini.com/about/
[6]New York State Department of Financial Services

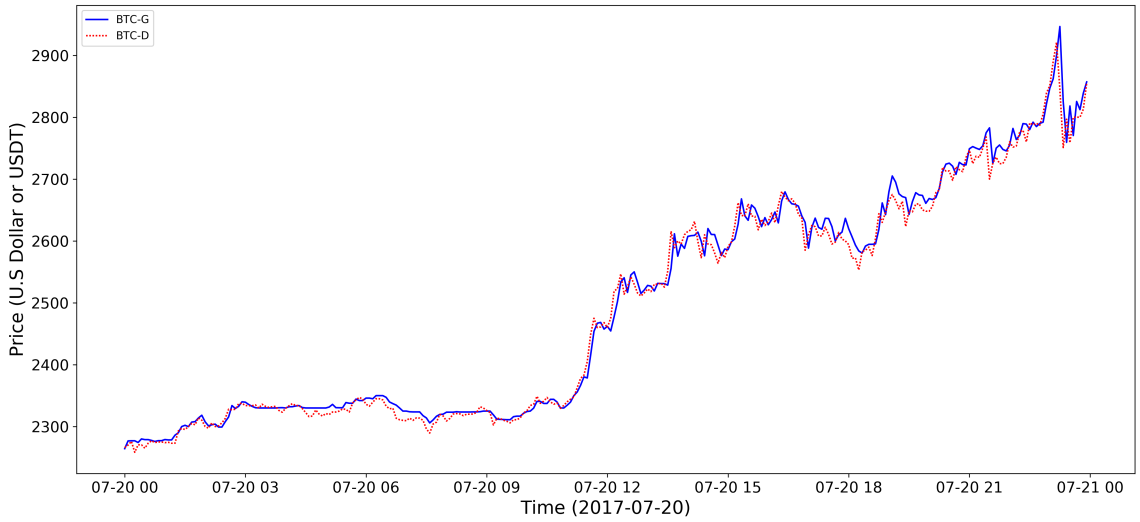

Figure 5: Price trajectory of BTC-D (dash line) and BTC-G (solid line) in the highest accumulated logreturn day, 20th July, 2017.

RiskBTC_Plot

equivalence is generated by so-called "1 USDT token is backed up by 1 U.S dollar" strategy. One of the pros of trading USDT is that all cryptocurrencies can be exchanged via USDT which results in better liquidity and more efficient prices, however, the USDT can be one of the risk factors for BTC. As Griffin and Shams (2018) discusses more about the functions of USDT.

The price in BTC-D is denoted by USDT, while the prices of BTC-G come from U.S. dollars trades. Price efficiency of those two exchanges can be evidenced by Fig.5 which shows the realized sample trajectory of BTC-D and BTC-G evolving closely in an extremely volatile day. Here we do not discuss more the risk from USDT but focus on characteristics of each of the processes.

3.3. Liquidity of Bitcoin Market

Bitcoin market is trading all-day and all-year globally akin to the foreign exchange market which prompt two issues that will be discussed below.

The first issue is the "calendar" effect which suggests that in some of the trading days when there are not enough trading activities, such as weekends or some national holidays, information can only be incorporated into prices in the very next "real" trading day. Removing those inactive days could reduce the "calender" effect but might also introduce biases.

We do not remove any trading days because many of the non-institutional investors who trade during non-business days in the cryptocurrency market. Also, program trading is

common in such "high-tech" centered market evidenced by Fig.6 in which we show that the very same logarithmic returns (rounded to 19 decimals) appears over 100 times in 2016 and it appears 7 times on March 3rd, 2016.

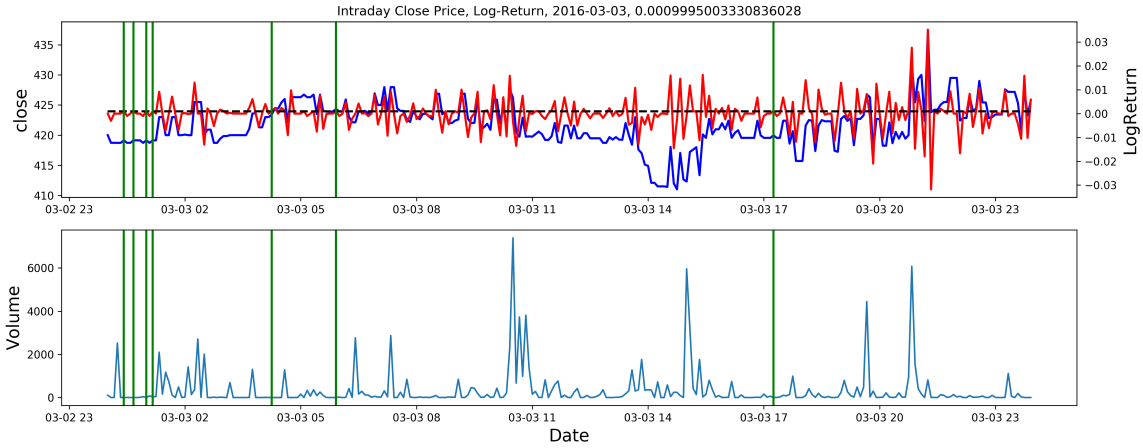

FIGURE 6: Same logarithmic return appears multiple times on March 3rd, 2016.
RiskBTC_Plot

The second issue comes from the definition of "day". As documented in previous literature, one could define a day as "21:05 GMT one night to 21:00 GMT next evening" (Andersen, Bollerslev, Diebold, and Labys (2001)). Truncating the "night periods" is also commonly seen in the literature.

The answer relies on whether Bitcoin market is a truly global market which has the same liquidity over the day or it is liquidity restricted for certain periods of the day. We justify the problem by investigating the trading volume pattern regarding BTC-D and BTC-G price processes. First, we define the Average Relative Trading Intensity $ARTI_{j\Delta}$ for each 5-minute interval $[(j-1)\Delta, j\Delta]$ to compare liquidity differences over time periods in Bitcoin market.

$$\begin{aligned} ARTI_{j\Delta} &\overset{def}{=} \frac{1}{N}\sum_{t=1}^{N} RTI_{t+j\Delta} \\ RTI_{t+j\Delta} &\overset{def}{=} \frac{vol_{t+j\Delta} - Minvol_{t+j\Delta,K}}{Maxvol_{t+j\Delta,K} - Minvol_{t+j\Delta,K}} \end{aligned} \tag{15}$$

Where $Minvol_{t+j\Delta,K} = \min_{k=-K\ldots,0,\ldots K} vol_{t+(j+k)\Delta}$ is the local minimum trading volume around $t+j\Delta$, Likewise $Maxvol_{t+j\Delta,K}$ is the local maximum trading volume value. Here we fix the window length $K = 288$ which can be referred to 48-hour ($\Delta = 5\text{-}minute$) relative trading intensity. And the N is the number of days in our sample.

$RTI_{t+j\Delta} \in [0,1]$ is essentially a rolling-window min-max transformation which assigns

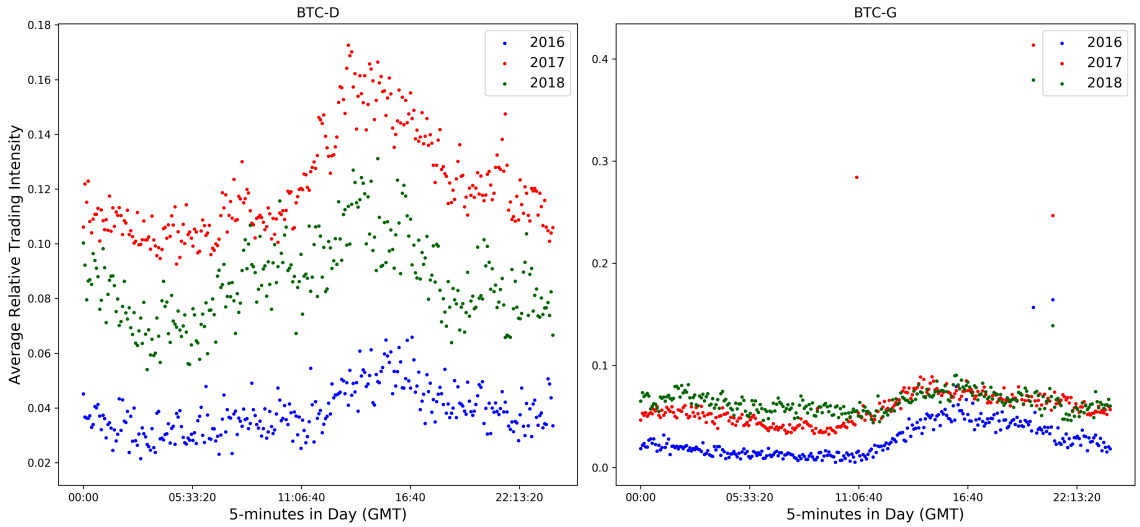

Figure 7: Average Relative Trading Intensity of BTC-D (left) and BTC-G (right) in 5-minute interval. Year of 2016, 2017, and 2019.

RiskBTC_Plot

the maximum values to 1 and the minimum values to 0. If the liquidity is almost equally distributed over time in day t, then $ARTI_{j\Delta}$ should evolve stably.

In this article, we define the day as 0:00 GMT to 23:55 GMT. Fig.7 shows the $ARTI_{j\Delta}, j = 1, \ldots, 288$ for BTC-D and BTC-G. As stated in the previous section, three out of four exchanges in our dataset are based on the U.S. Consistently, the active trading time period for both BTC-D and BTC-G are both around 15:00 GMT which is the likely the trading hour of the U.S market. However, in our dataset, one can see that many trades were also generated during European, Asian market trading hours. It would be biased if one takes account only the U.S. market trading hours. Despite the fact that some $ARTI$ extreme outliers exist for BTC-G, we still see similar trading volume pattern between those two prices processes.

3.4. Dynamics of Realized Variance

The subsection discusses the dynamics of variance estimates in 3 aspects including descriptive statistics, empirical distribution, and series autocorrelation.

The descriptive statistics of continuous component C and TC suggest that the discontinuities do not contribute to the risk too much. As definition in section 2.2, $(T)C$ are the differences between RV and $(T)J$. Closer $(T)C$ to RV, lower contribution from $(T)J$. Averagely, jumps contribute to risk up to 6.8% for BTC-D, and up to 17.2% for BTC-G. Percentile statistics give consistent results.

As discussed previously, RV can be decomposed into positive and negative estima-

tors $RSV^{+(-)}$, one can see that $mean(RV) \approx mean(RSV^+) + mean(RSV^-)$ from Tab.2. Take BTC-D for example, the mean value of those estimators are $mean(RV) \approx 1.16$, $mean(RSV^+) \approx 0.57$, and $mean(RSV^-) \approx 0.59$. And ADF unit root test suggests that most estimators do not contain unit root at 5% significant level.

Table 2: Summary Statistics For Bitcoin Annualized Daily (Semi-)Realized Variance

Panel A: BTC-D								
	RV	RSV^+	RSV^-	$\log(RV)$	$\log(RSV^+)$	$\log(RSV^-)$	C	TC
mean	1.16	0.57	0.59	−0.60	−1.32	−1.30	1.12	1.08
std	2.05	1.02	1.05	1.20	1.22	1.23	2.06	2.01
min	0.02	0.01	0.01	−3.98	−4.88	−4.51	0.01	0.01
5%	0.08	0.04	0.04	−2.54	−3.29	−3.27	0.06	0.05
50%	0.56	0.27	0.26	−0.58	−1.31	−1.33	0.51	0.47
95%	3.70	1.81	2.06	1.31	0.59	0.72	3.70	3.69
max	26.07	13.28	12.80	3.26	2.59	2.55	26.07	26.07
skewness	5.59	5.78	5.41	0.06	0.04	0.10	5.60	5.73
kurtosis	43.38	46.24	40.12	−0.04	−0.03	−0.15	43.40	45.86
acf(1)	0.53	0.51	0.52	0.79	0.78	0.77	0.53	0.56
acf(7)	0.17	0.16	0.17	0.58	0.58	0.57	0.17	0.18
acf(30)	0.11	0.10	0.11	0.38	0.37	0.38	0.12	0.13
acf(100)	0.06	0.06	0.06	0.23	0.23	0.23	0.06	0.07
ADF	-3.16^{**}	-3.22^{**}	-3.12^{**}	-4.36^{***}	-4.34^{***}	-4.42^{***}	-3.12^{**}	-3.10^{**}
Panel B: BTC-G								
	RV	RSV^+	RSV^-	$\log(RV)$	$\log(RSV^+)$	$\log(RSV^-)$	C	TC
mean	0.93	0.45	0.49	−0.92	−1.66	−1.64	0.85	0.77
std	1.76	0.84	0.98	1.32	1.32	1.37	1.64	1.55
min	0.01	0.00	0.00	−4.88	−5.51	−5.63	0.00	0.00
5%	0.04	0.02	0.02	−3.15	−3.90	−4.00	0.03	0.02
50%	0.40	0.19	0.19	−0.91	−1.65	−1.64	0.33	0.28
95%	3.17	1.53	1.73	1.15	0.42	0.55	3.09	2.95
max	21.99	11.78	14.52	3.09	2.47	2.68	21.99	21.99
skewness	5.86	6.32	6.85	−0.04	−0.04	−0.01	5.73	6.21
kurtosis	47.28	59.42	68.92	−0.10	−0.14	−0.19	48.03	57.88
acf(1)	0.42	0.45	0.35	0.74	0.73	0.71	0.47	0.50
acf(7)	0.13	0.14	0.11	0.49	0.51	0.47	0.16	0.19
acf(30)	0.09	0.09	0.07	0.26	0.26	0.25	0.12	0.14
acf(100)	0.03	0.04	0.02	0.11	0.11	0.11	0.03	0.04
ADF	-3.03^{**}	-3.12^{**}	-4.89^{***}	-5.06^{***}	-3.61^{***}	-5.27^{***}	-2.95^{**}	-2.77^{*}

***: 1% significance, **: 5% significance, *: 10% significance

The empirical kernel density estimation of $\log(RV)$, $\log(RSV^{+(-)})$ and $\log((T)C)$ are shown in Fig.8. Each subfigure in Fig.8 has normal distribution probability density function, normal PDF, shadowed in the background to contrast the empirical density. The two parameters, μ, σ, for normal PDF are taken from the mean and standard deviation values of the corresponding estimator. For example, the BTC-D has $mean(\log(RV)) = -0.12$, $std(\log(RV)) = 0.96$, the normal PDF is $\varphi(x| - 0.12, 0.96) = (2\pi * 0.96)^{-1/2} \exp(-\frac{(x+0.12)^2}{2*0.96^2})$.

Consistent with the results that skewness and excessive kurtosis of those logarithmic forms are all close to 0 shown in Tab.2, we can see the empirical density of those estimators are very close to the normal distribution in the background. Consistent with Andersen, Bollerslev, Diebold, and Ebens (2001) and Bollerslev, Hood, Huss, and Pedersen (2018), all the RV-type estimators are likely log-normally distributed .

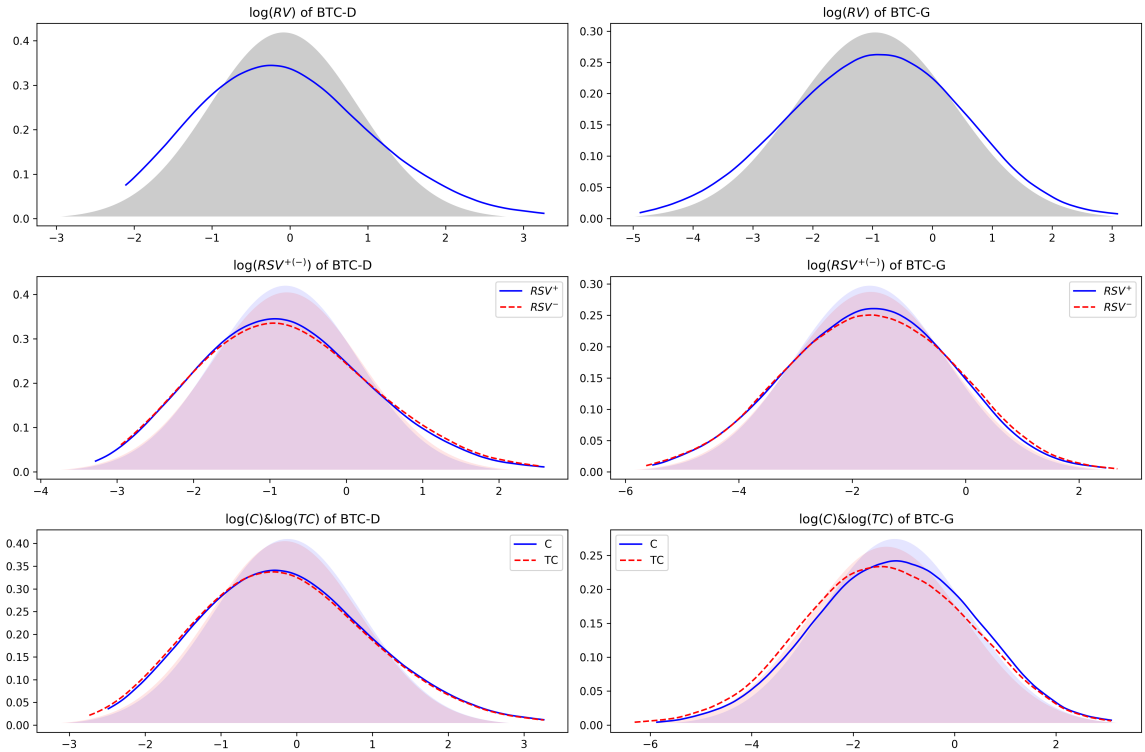

Figure 8: Kernel density estimation on annualized unconditional daily logarithmic estimators for BTC-D (left column) and BTC-G (right column). Shadows in the background represent normal probability density function with corresponding empirical local and scale parameters of estimators

RiskBTC_Plot

Autocorrelation is the key for time series forecasting, particularly, $\log(RV)$ is characterized as long memory in previous literature. In Tab.2, the autocorrelation function is computed with $lags = 1\text{-}day, 7\text{-}days, 30\text{-}days, 100\text{-}days$, noted as acf(1), acf(7), acf(30), acf(100). On one hand, we see strong autocorrelation of all the RV-type estimators at lags of 1-day and 7-days for both BTC-D and BTC-G. On the other hand, the decay rates on autocorrelation may vary between different exchanges for the same crypto asset. One can see quite different decay rate between of BTC-D and BTC-G. BTC-G has a stronger and more sustained long-memory effect which is aligned with ACF results in Tab.2. Furthermore, the logarithmic form of those processes shows a clearly stronger serial dependency structure. Each subfigure in Fig.9 shows that the dynamics of dependencies behave in a similar pattern.

3.5. Dynamics of Jumps

Recall that we construct six estimators to measure jumps, J, TJ, and $(T)J^{+(-)}$ in Sec.2. Summary statistics of those estimators are described in Tab.3 and Fig.10 depicts how their intensity evolve over time. $J(\alpha)$ and $TJ(\alpha)$ are evaluated under $\alpha = 99.99\%$ confidence

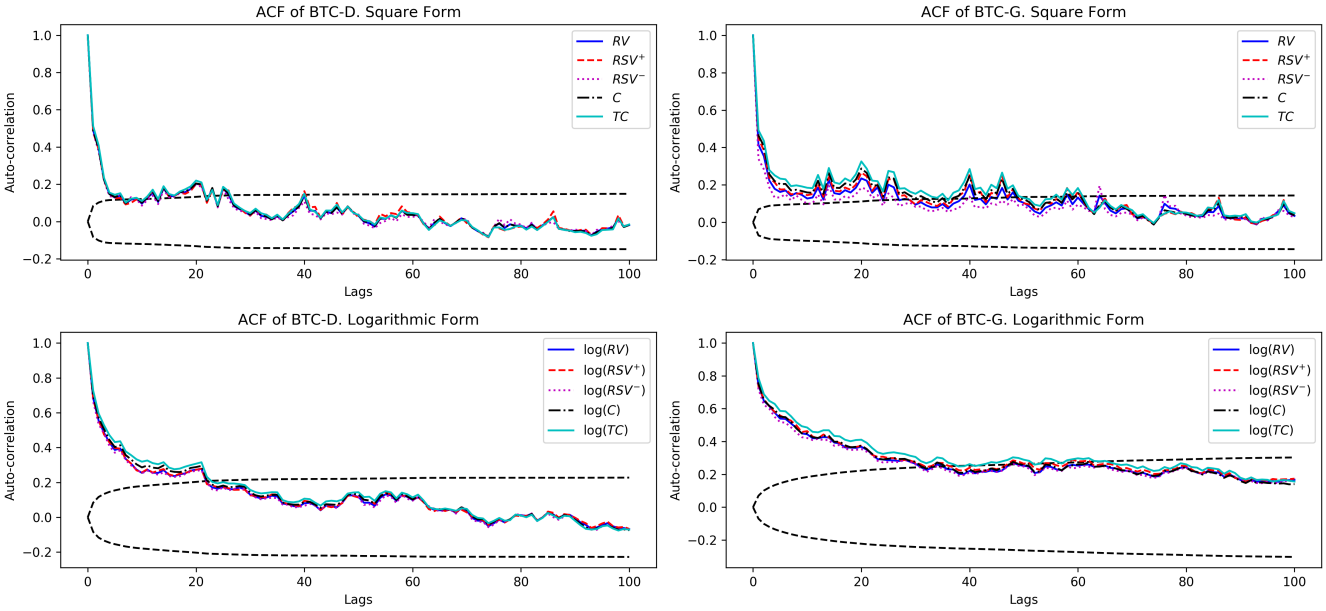

Figure 9: Autocorrelation function of estimators in square and logarithmic forms for BTC-D (left column) and BTC-G (right column)

RiskBTC_Plot

level. The average intensity of jump components is approximate $(T)J(\alpha) \approx (T)J^{+} + (T)J^{-}$, the error is partially caused by the lack of significance test on signed jumps $(T)J^{+(-)}$. The size and quantity of negative jumps $(T)J^{-}$ are almost equal to that of positive jump $(T)J^{+}$.

Jumps appear far more frequently in Bitcoin market than in any other developed markets comparing the results documented by pervious researches using similar approaches. From our empirical results in Tab.3, 25% and 51% of days are detected with jumps using J estimator for BTC-D and BTC-G, respectively. And those numbers are up to 39% and 68% by TJ estimator. Corsi, Pirino, and Reno (2010) shows that for the most liquid six stocks of S&P500 8.3% of the 1256 sample days are with jumps by $TJ(\alpha = 99.9\%)$. Andersen, Bollerslev, and Diebold (2007) does experiments on various financial assets including DM/$, S&P 500 and U.S T-Bond by using J estimator and 8.3%, 5.1% and 7.6% of all days are been detected with jumps, correspondingly.

Nevertheless, the simple equal-weighted portfolio, BTC-D, reduces the size and quantity of jumps significantly. Comparing the two panels in Tab.3, more jumps are detected in BTC-G than in BTC-D. The price process of BTC-D is constructed by weighting prices from multiple exchanges equally, thus jumps detected by high-frequency data can be canceled out from such construction. For example, a market event happened, exchanges prices react at a different speed, say one exchange's price reacts simultaneously and another exchange reacts a few minutes later, then such jump in synthetic price is "smoothed out". Hence, one can see

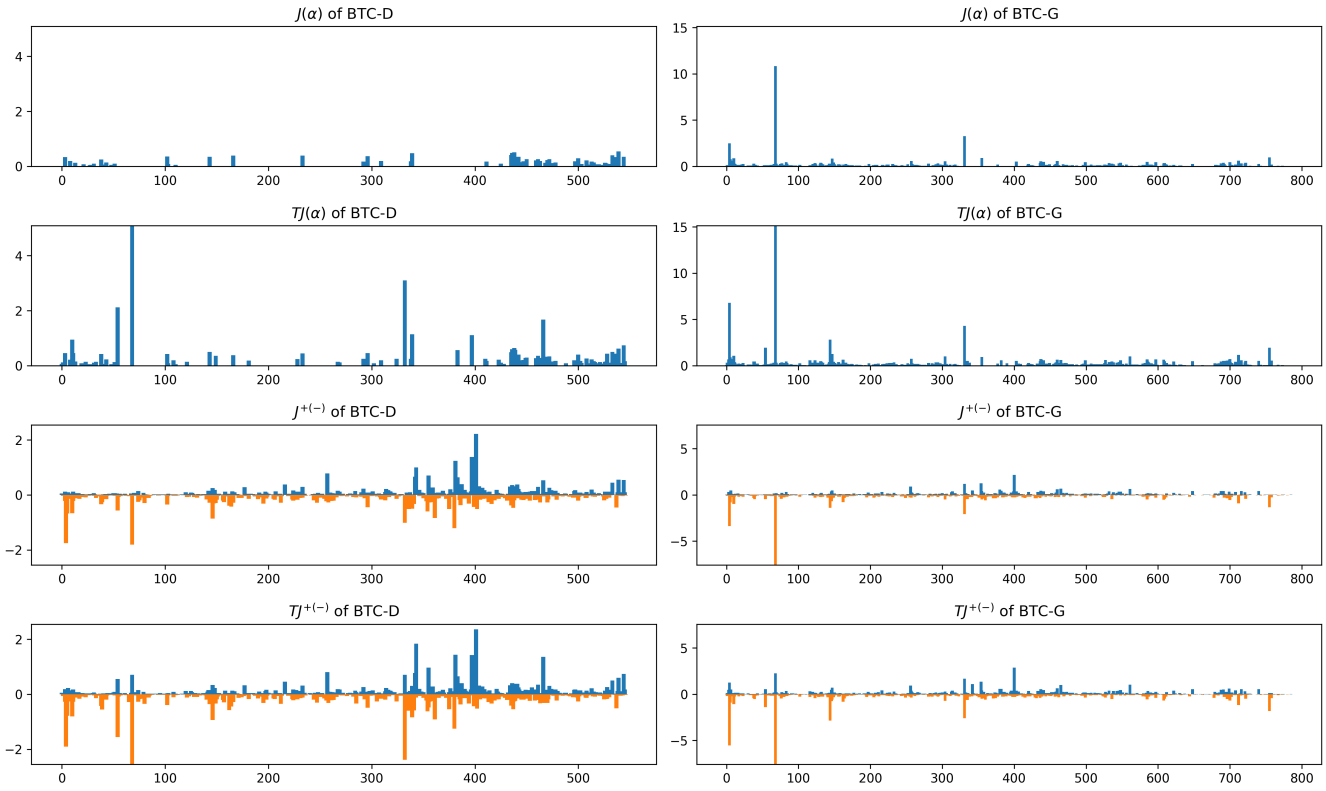

Figure 10: Jump components decomposed from realized variance of BTC-D (left column) and BTC-G (right column). Panels from top to bottom are $J(\alpha)$, $TJ(\alpha)$, $J^{+(-)}$, and $TJ^{+(-)}$ defined in Sec.2. $\alpha = 99.99\%$ is the confidence level.

RiskBTC_Plot

that, by TJ estimator, 39% of days in BTC-D sample are entangled with jumps while 68% of days are found with jumps in BTC-G. Furthermore, more extreme jumps appear in BTC-G than in BTC-D by percentile statistics. BTC-G is more positive skewed and leptokurtic than BTC-D in terms of all jump estimators, for example, $skewness(\text{BTC-D}, J) = 1.69$ versus $skewness(\text{BTC-G}, J) = 15.90$ and $kurtosis(\text{BTC-D}, J) = 2.55$ versus $kurtosis(\text{BTC-G}, J) = 290.20$.

By the threshold smoothing method $TBPV$, much more jumps can be detected from $TJ(\alpha)$ estimator, or in other words, the threshold method has a stronger detection ability on the jumps in Bitcoin market. In BTC-D, 39% of all days with jumps by TJ comparing 25% by J, and the statistics are 68% against 51% in BTC-G. Also, TJ component is more intensive than J component. Especially, we can see TJ has much larger value at 95-percentile and maximum, this may suggest that some of the large size jumps or consecutive jumps are missed in J.

Table 3: Summary Statistics For Bitcoin Jump Components

Panel A: BTC-D						
	$J(\alpha)$	$TJ(\alpha)$	J^+	J^-	TJ^+	TJ^-
prop.†	0.25	0.39	0.68	0.73	0.76	0.79
mean	0.12	0.20	0.08	0.09	0.09	0.11
std	0.14	0.40	0.17	0.17	0.21	0.25
min(%)	0.83	0.92	0.01	0.01	0.02	0.03
5%(%)	1.00	1.00	0.30	0.35	0.36	0.46
50%	0.07	0.09	0.03	0.03	0.03	0.04
95%	0.40	0.64	0.3	0.32	0.34	0.39
max	0.66	5.09	2.22	1.81	2.36	4.39
skewness	1.69	7.28	6.37	5.28	5.80	9.46
kurtosis	2.55	73.22	56.2	40.47	43.31	131.43
Panel B: BTC-G						
	$J(\alpha)$	$TJ(\alpha)$	J^+	J^-	TJ^+	TJ^-
prop.	0.51	0.68	0.75	0.81	0.83	0.87
mean	0.17	0.24	0.08	0.12	0.11	0.15
std	0.56	0.76	0.16	0.45	0.23	0.56
min	0.30%	0.34%	0.01%	0.00%	0.00%	0.02%
5%	0.90%	1.00%	0.24%	0.33%	0.32%	0.38%
50%	0.08	0.11	0.04	0.04	0.04	0.05
95%	0.44	0.65	0.34	0.37	0.38	0.44
max	10.82	15.14	2.16	10.71	2.86	12.87
skewness	15.90	14.40	6.45	19.27	6.77	17.33
kurtosis	290.20	259.24	61.08	437.7	62.06	368.50

Confidence level $\alpha = 99.99\%$, threshold coefficient constant $c_\theta = 3$. All statistics exclude zero or insignificant observations.

4. Accounting Separated Jumps in Realized Variance Modelling

4.1. Conditional Distribution of Realized Variance

One of the motivations of jump detection is observing how jump shocks the distribution of future RV, i.e the conditional distribution of RV. Each subfigure in Fig.11 shows the distribution of RV unconditional, conditional on having (T)J, and conditional on having no-(T)J. Figures in Fig.11 show consistently that if a jump being detected at day t, the distribution of next day's $\log(RV_{t+1})$ would shift negatively implying that jump possibly reduce risk on the next day. On the other hand, if there is no jump being detected, the bitcoin market is, on average, more volatile in the next day.**[add figures for h=7,30 in appendix]** In this article, by inserting the jump measures into the HAR model, we will further discuss how jumps impact realized volatility in the future.

4.2. Realized Variance and Jump Estimators Construction

In the section2, we briefly illustrate the estimators used in this article including the realized (semi-)variance RV, $RSV^{+(-)}$ and the jump estimators $(T)J^{+(-)}$. Here we would

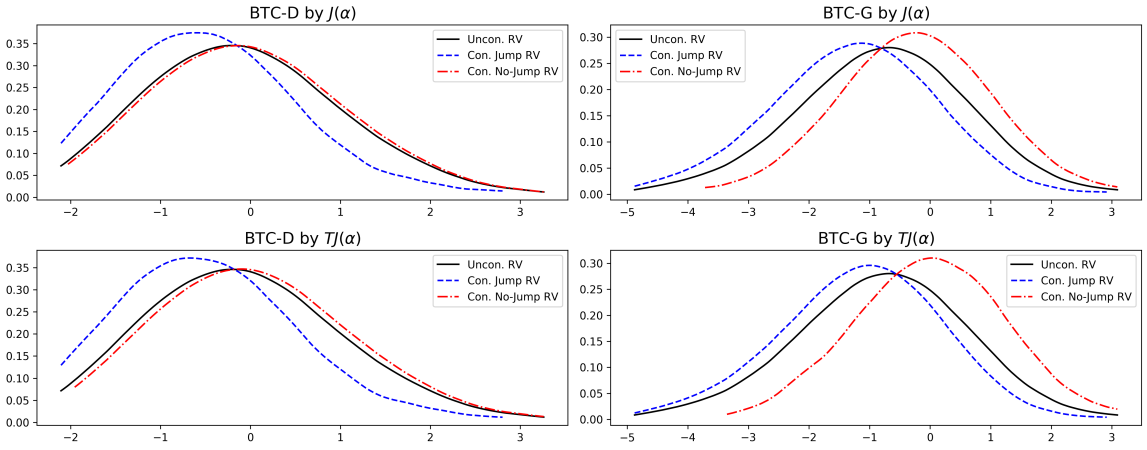

FIGURE 11: Distribution of **BTC-D** and **BTC-G** $\log(RV_{t+1})$ conditioning on jumps/no-jumps appear on day t.

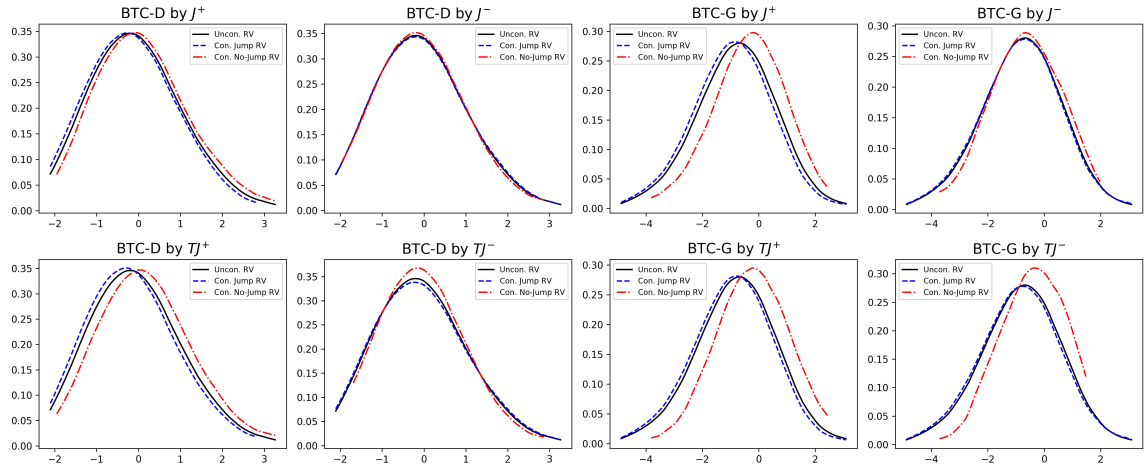

FIGURE 12: Distribution of **BTC-D** and **BTC-G** $\log(RV_{t+1})$ conditioning on signed-jumps/no-signed-jumps appear on day t.

like to clarify the notation of each estimator in different forms and over different periods.

For simplicity, any of the estimators over a longer period is computed by averaging its daily estimate over the period. The averaging method not only has incorporated information included in different periods but also ensure estimates over different periods having the same scale. Given an daily estimator $\hat{Y}_\tau$, its corresponding average estimator is defined as:

$$\hat{Y}_{\tau_1,\tau_2} = \frac{1}{\tau_2 - \tau_1} \sum_{\tau=\tau_1+1}^{\tau_2} \hat{Y}_\tau \tag{16}$$

Take RV for example, all the empirical results are based on the annualized unconditional

daily realized variance RV_{t+1} in (2). The longer horizon estimator, $RV_{t,t+7}$, is average of annualized daily estimates $RV_{t,t+7} = \frac{1}{6}\sum_{\tau=t+1}^{t+7} RV_\tau$.

We specially denote the daily lagged, weekly lagged and monthly lagged estimators for further use as follows.

$$\begin{aligned} \text{Daily estimator}, \hat{Y}_D &\stackrel{def}{=} \hat{Y}_{t-1,t} \\ \text{Weekly estimator}, \hat{Y}_W &\stackrel{def}{=} \hat{Y}_{t-7,t-1} \\ \text{monthly estimator}, \hat{Y}_M &\stackrel{def}{=} \hat{Y}_{t-30,t-7} \end{aligned} \tag{17}$$

Those three stepwise estimators will be employed in the latter HAR model which captures the footprint of $RV's$ long memory property.

To incorporate nonlinearity, we also use estimators in logarithmic form $\log(\hat{Y})$, for example $\log(RV)$, $\log(J+1)$. Economically, the squared form RV (realized variance) is of our interest, thus any forecasting result computed from the logarithmic form is transformed back to squared form for comparison purpose.

4.3. HAR Models

The long-memory dependency structure of the variance process is crucial in forecasting according to the previous literature in which people use different ARCH, ARMA, and stochastic volatility models to capture such property. As the forecasting models are developed more and more complicated, Corsi (2009) introduce the Heterogenous AutoRegression model, namely **HAR**, which has advantages in three folds. First, it is a parameter parsimonious volatility regression model that can be constructed easily with lagged regressors over different horizons. And it captures the long-memory effect and shows good forecasting performance comparing with those complicated models. Finally, HAR can be extended by using any other relevant estimators, for example, the jump components. Such extensibility allows one to investigate a wide range of effects on RV.

Here we would study the improvement of forecast accuracy from different models instead of absolute forecast accuracy, hence follow many of the literature on realized volatility forecasting, HAR-RV and its extensive models are used.

The general form of HAR is shown in (18). The dependent variable $RV_{t,t+h}$ is estimated over three different horizons, $h = 1, 3, 7$. There are two sets of explanatory variables, $X_{\dot{RV}}$ and X_j, which represent multiperiod lagged realized (semi-)variance estimators and jump estimators, respectively. Economic intuitively, we focus on daily, weekly and monthly lagged

estimators which are defined in 17. Hence, the explanatory variables, for example, can be written explicitly using estimators in Sec.4.2, $X_{\dot{RV}}^{\top} = \left(\dot{RV}_D, \dot{RV}_W, \dot{RV}_M\right)$ and $X_{\dot{J}}^{\top} = \left(\dot{J}_D, \dot{J}_W, \dot{J}_M\right)$.

All coefficients, $\beta_{\dot{RV}} = (\beta_D, \beta_W, \beta_M)^{\top}$ and $\beta_J = (\beta_{JD}, \beta_{JW}, \beta_{JM})^{\top}$, are estimated by OLS. To adjust the possible serial correlation and heteroskedasticity of the error term, we use Newey-West covariance matrix estimator with 7, 14 and 60 lags for daily, weekly and monthly forecast horizon, respectively. Note that all the jump estimators are relied on $\alpha = 0.9999$ and $c_\theta = 3$.

$$RV_{t,t+h} = \alpha + X_{\dot{RV}}^{\top}\beta_{\dot{RV}} + X_{\dot{J}}^{\top}\beta_{\dot{J}} + \varepsilon_{t,t+h}, \quad t = 1, \ldots, T \tag{18}$$

The basic version **HAR** model is formulated by letting $\dot{RV} = RV$, and removing $\dot{J}$ components in (18), i.e $RV_{t,t+h} = \alpha + X_{RV}^{\top}\beta_{RV} + \varepsilon_{t,t+h}$. HAR model is the simplest and roughest model in this article.

Based on the HAR model, one could construct model that accounts jump components by simply adding jump component by which the method we have discussed in section 2, i.e let $\dot{RV} = RV$ and $\dot{J} = J$, thus $RV_{t,t+h} = \alpha + X_{RV}^{\top}\beta_{RV} + X_J^{\top}\beta_J + \varepsilon_{t,t+h}$. We call this Realized Variance Jump model **RVJ**.

Similarly, the Realized Variance Thresholded Jump model **RVTJ** accounts the thresholded jump components that can be expressed by having $\dot{RV} = RV$ and $\dot{J} = TJ$, i.e $RV_{t,t+h} = \alpha + X_{RV}^{\top}\beta_{RV} + X_{TJ}^{\top}\beta_{TJ} + \varepsilon_{t,t+h}$.

Furthermore, one can construct the Realized Variance Signed Jump model **RVSJ** and the Realized Variance Signed Thresholded Jump model **RVSTJ** by decomposing the jump components in RVJ and RVTJ model into signed jump components. To be more specifically, RVSJ can be formulated as $RV_{t,t+h} = \alpha + X_{RV}^{\top}\beta_{RV} + X_{J^+}^{\top}\beta_{J^+} + X_{J^-}^{\top}\beta_{J^-} + \varepsilon_{t,t+h}$. And RVSTJ is $RV_{t,t+h} = \alpha + X_{RV}^{\top}\beta_{RV} + X_{TJ^+}^{\top}\beta_{TJ^+} + X_{TJ^-}^{\top}\beta_{TJ^-} + \varepsilon_{t,t+h}$. Those two models are finer calibrated and allow different impacts of positive and negative jumps on future realized variance.

On the other hand, one can also decompose the realized variance estimators. The Realized SemiVariance model **RSV** is constructed by decomposing RV in HAR model with RSV, i.e $RV_{t,t+h} = \alpha + X_{RSV^+}^{\top}\beta_{RSV^+} + X_{RSV^-}^{\top}\beta_{RSV^-} + \varepsilon_{t,t+h}$.

With analogous arguments, two finest models, the Realized SemiVariance Signed Jump model **RSVSJ**, and the Realized SemiVariance Signed Thresholded Jump model **RSVSTJ** are constructed via the full decomposition method which accounts both the positive/negative variance and jumps. i.e

$$RV_{t,t+h} = \alpha + X_{RSV^+}^\top \beta_{RSV^+} + X_{RSV^-}^\top \beta_{RSV^-} + X_{J^+}^\top \beta_{J^+} + X_{J^-}^\top \beta_{J^-} + \varepsilon_{t,t+h}$$
$$RV_{t,t+h} = \alpha + X_{RSV^+}^\top \beta_{RSV^+} + X_{RSV^-}^\top \beta_{RSV^-} + X_{TJ^+}^\top \beta_{TJ^+} + X_{TJ^-}^\top \beta_{TJ^-} + \varepsilon_{t,t+h} \quad (19)$$

As stated in Sec.4.2, those estimators can be transformed into logarithmic form and then used to construct logarithmic HAR-type models which capture the nonlinearity. Also, the logarithmic forecasting model ensures forecasts values RV to be positive. Here we simply define the logarithmic HAR-type models by replacing all estimators with the logarithmic form.

$$\log\left(RV_{t,t+h}\right) = \alpha + \log\left(X_{\dot{RV}}\right)^\top \beta_{\dot{RV}} + \log\left(X_j\right)^\top \beta_j + \varepsilon_{t,t+h}, \quad t = 1, \ldots, T \quad (20)$$

Where, for example, $\log\left(X_{\dot{RV}}\right)^\top = \Big(\log(\dot{RV}_D), \log(\dot{RV}_W), \log(\dot{RV}_M)\Big)$.

Note that here we ensure the logarithmic form of jump estimators to be positive by $\log\left(X_j\right)^\top = \Big(\log(\dot{J}_D + 1), \log(\dot{J}_W + 1), \log(\dot{J}_M + 1)\Big)$.

To summarize it up, we have 8 forecasting models including **HAR, RVJ, RVTJ, RSV, RSVSJ, RSVSTJ**. Also, we will test 2 forms of each model, namely **square form** and **logarithmic form**.

4.4. In-Sample Fitting Analysis of HAR-Type Models

This subsection discusses the results of the full-sample fitting. To analyze how each explanatory variable affects future RV, we fit each of the HAR models with full sample, i.e from the start of 2017 until the Middle of 2019[7], named as full-sample fitting. For the roughest estimators, realized variance RV, all models show consistently that the one-day lagged estimator RV_D have a significant positive impact on RV_{t+1} which is the short horizon forecasting case. And the significance of such effect decreases as the estimator lagged more, i.e for RV_W and RV_M. As the logarithmic form of that regression would capture certain nonlinearity between predictors and dependent variable, it is no surprise to find that the coefficients in logarithmic form results are likely to be more significant than of those in square form.

The regression results get controversial and obscured after the decomposition of estimators. As RV is decomposed into upside risks RSV_D^+ (good volatility) and downside risks RSV_D^- (bad volatility), the BTC-D results in Tab.4 indicate that the bad volatility increases risk of the next day and the good volatility shows much less significant impact. However,

[7]The sample date lasts until July 2019 for BTC-D and May 2019 for BTC-G

results of BTC-G in Tab.5 show otherwise. In the cases of modelling the decomposed jumps (good jumps and bad jumps) with RV and RSV estimators, the higher good jumps more likely to reduce risk of the next day. While it is ambiguous to draw any robust conclusion on the impact of bad jumps. More puzzling results would be found in the sample period is changed.

Despite the parameter estimations changing over time using rolling window described in the next subsection, it is worth looking into the average impacts of those predictors as some of the contrary facts motivate us to implement the rolling window method.

The fast-changing Bitcoin market is not only characterized by high volatility but also observed with market structure changes. When market structure changes intensively, any conclusion could be ambiguous and confusing if it is drawn only by comparing models using the out-of-sample forecast as the forecasting period could deviate from the fitting period substantially. By allowing parameters changing over time, more reasonable comparisons can be obtained.

The adaptive method used mimics an investor who updates the forecasting model based on the most recent information. A simple situation is assuming that such updates are based on a fixed amount of lagged information. The window size T of the adaptive HAR models employed here is 90-days, i.e models are estimated by using past 90-days samples. And all the models are re-estimated every day. After re-estimation of each day, out-of-sample forecasts are performed in horizons $h = 1, 7, 30$, spontaneously. As a result, we re-estimate each model 744-times for BTC-D and 763-times for BTC-G.

The left subfigure of each panel in Fig.13 shows that RV_D has significant positive impact on $RV_{t,t+1}$ consistent with results in Tab.4 and 5. One can predict that the next trading day $t + 1$ would be riskier after experiencing high volatility in day t.

The upside and downside risk estimators play two different roles in forecasting over time. Recall that the RSV model is constructed based on the HAR model by decomposing RV into upside/downside risk RSV^+ and RSV^-. Each panel in Fig.13 shows the how β_D^+ and β_D^- evolve corresponding with the t-values denoted by blue dots. Over the 2 years, the upside risk coefficients β_D^+ evolve as a u-shape curve, and oppositely the pattern of the downside risk coefficients β_D^- are similar to an n-shape curve.

Obviously, the impact of upside/downside risk links to the market status. Specifically, the downside risk plays a more important role in forecasting RV during volatile periods. For example in the period from late-2017 to mid-2018 when Bitcoin price reached the peak price around 20,000 U.S. dollars in December 2017 and then was plunged more than 50%. During the volatile period, on one hand, RSV_D^- has a significant positive impact on the next day realized variance which implies that the downside risks would cause higher volatility. On the

Table 4: Regression Results of Full-Sample Fitting, **BTC-D**

h=1	**Square form**							**Logarithmic form**						
	α	$\beta_D^{(+/-)}$	$\beta_W^{(+/-)}$	$\beta_M^{(+/-)}$	$\beta_{JD}^{(+/-)}$	$\beta_{JW}^{(+/-)}$	$\beta_{JM}^{(+/-)}$	α	$\beta_D^{(+/-)}$	$\beta_W^{(+/-)}$	$\beta_M^{(+/-)}$	$\beta_{JD}^{(+/-)}$	$\beta_{JW}^{(+/-)}$	$\beta_{JM}^{(+/-)}$
HAR	0.175	0.437	0.100	0.311				−0.122	0.568	0.236	0.132			
	(2.460)	(6.284)	(2.119)	(2.722)				(−4.341)	(15.758)	(5.387)	(2.797)			
RVJ	0.335	0.430	0.089	0.292	0.680	−0.179	−4.216	−0.053	0.570	0.227	0.116	−0.426	−0.595	−1.500
	(2.953)	(6.466)	(1.862)	(2.523)	(0.781)	(−0.195)	(−2.494)	(−1.335)	(15.879)	(5.002)	(2.434)	(−1.094)	(−1.151)	(−1.789)
RVTJ	0.271	0.457	0.089	0.292	−0.476	−0.046	−0.538	−0.006	0.600	0.225	0.096	−0.574	−0.534	−0.489
	(1.696)	(6.470)	(1.743)	(2.452)	(−2.303)	(−0.112)	(−0.489)	(−0.147)	(17.108)	(4.745)	(2.164)	(−3.053)	(−1.932)	(−1.35)
RVSJ†					−1.071	−0.647	−3.063					−0.514	−1.308	0.299
	0.382	0.431	0.065	0.521	(−1.958)	(−0.572)	(−2.095)	0.115	0.581	0.315	0.133	(−2.139)	(−2.503)	(0.448)
	(2.464)	(3.785)	(0.765)	(3.224)	0.800	1.126	−4.111	(1.171)	(13.658)	(4.817)	(1.792)	−0.134	−0.91	−0.943
					(0.515)	(0.683)	(−1.803)					(−0.418)	(−1.301)	(−0.855)
RVTSJ†					−1.357	−0.925	−1.547					−0.602	−1.245	0.312
	0.305	0.495	0.089	0.363	(−3.593)	(−1.063)	(−1.210)	0.097	0.605	0.301	0.103	(−3.211)	(−3.225)	(0.555)
	(1.994)	(5.193)	(1.134)	(3.141)	−0.086	0.798	−0.303	(1.195)	(13.871)	(4.841)	(1.778)	−0.223	−0.334	−0.455
					(−0.138)	(1.085)	(−0.198)					(−0.98)	(−0.768)	(−0.746)
RSV†		−0.161	−0.803	−0.217					0.202	0.045	0.069			
	0.170	(−0.379)	(−1.599)	(−0.27)				0.534	(2.999)	(0.434)	(0.519)			
	(2.257)	1.008	0.986	0.834				(14.328)	0.375	0.182	0.057			
		(2.417)	(1.877)	(0.989)					(5.939)	(1.719)	(0.421)			
RSVSJ†		0.839	−1.858	0.094	−1.608	2.091	−2.449		0.233	0.126	−0.005	−0.319	−1.228	0.574
	0.407	(0.615)	(−1.069)	(0.023)	(−0.909)	(0.883)	(−0.41)	0.833	(3.025)	(1.027)	(−0.027)	(−1.284)	(−2.255)	(0.728)
	(2.364)	0.023	1.979	0.948	1.381	−1.968	−4.853	(6.268)	0.349	0.182	0.137	−0.157	−0.989	−1.279
		(0.015)	(1.084)	(0.231)	(0.473)	(−0.471)	(−0.682)		(4.473)	(1.379)	(0.671)	(−0.456)	(−1.23)	(−0.902)
RSVSTJ†		−1.603	−1.049	3.722	1.095	0.623	−5.764		0.255	0.212	−0.005	−0.454	−1.367	0.542
	0.317	(−1.376)	(−0.629)	(0.656)	(0.827)	(0.399)	(−0.874)	0.786	(3.299)	(1.713)	(−0.029)	(−2.164)	(−3.09)	(0.755)
	(2.14)	2.568	1.176	−2.905	−2.307	−0.446	3.128	(7.646)	0.353	0.079	0.104	−0.264	−0.178	−0.586
		(2.161)	(0.682)	(−0.52)	(−1.657)	(−0.228)	(0.482)		(4.557)	(0.624)	(0.54)	(−1.106)	(−0.363)	(−0.746)

†: Results from positive (above) and Negative (below) estimators are separated by horizontal lines.

Table 5: Regression Results of Full-Sample Fitting, **BTC-G**

h=1	**Square form**							**Logarithmic form**						
	α	$\beta_D^{(+/-)}$	$\beta_W^{(+/-)}$	$\beta_M^{(+/-)}$	$\beta_{JD}^{(+/-)}$	$\beta_{JW}^{(+/-)}$	$\beta_{JM}^{(+/-)}$	α	$\beta_D^{(+/-)}$	$\beta_W^{(+/-)}$	$\beta_M^{(+/-)}$	$\beta_{JD}^{(+/-)}$	$\beta_{JW}^{(+/-)}$	$\beta_{JM}^{(+/-)}$
HAR	0.178	0.333	0.163	0.326				−0.182	0.532	0.262	0.127			
	(2.315)	(4.560)	(3.016)	(2.654)				(−5.267)	(16.773)	(6.793)	(2.856)			
RVJ	0.278	0.379	0.175	0.273	−0.493	−0.500	−0.372	−0.048	0.528	0.301	0.107	−0.436	−0.863	−0.51
	(3.591)	(5.110)	(2.677)	(2.251)	(−2.676)	(−1.977)	(−0.824)	(−0.981)	(16.499)	(7.329)	(2.462)	(−2.17)	(−3.112)	(−1.425)
RVTJ	0.302	0.393	0.171	0.259	−0.333	−0.241	−0.266	−0.002	0.55	0.313	0.071	−0.412	−0.643	−0.232
	(3.94)	(4.732)	(2.446)	(2.045)	(−2.106)	(−1.596)	(−0.877)	(−0.032)	(16.423)	(7.01)	(1.525)	(−2.452)	(−3.275)	(−0.835)
RVSJ†	0.513	0.424	0.343	0.414	−1.347	−3.877	−3.297	0.254	0.543	0.376	0.158	−0.584	−1.875	−0.954
	(4.279)	(4.243)	(2.858)	(2.21)	(−2.356)	(−2.565)	(−1.467)	(1.828)	(13.176)	(6.949)	(2.351)	(−1.828)	(−3.856)	(−0.896)
					−0.502	−0.434	−0.605					−0.252	−0.805	−0.673
					(−1.769)	(−1.771)	(−1.300)					(−0.872)	(−2.862)	(−1.553)
RVTSJ†	0.519	0.437	0.304	0.348	−1.211	−2.857	−2.372	0.226	0.555	0.373	0.113	−0.658	−1.64	−0.52
	(5.051)	(4.347)	(2.745)	(2.199)	(−2.857)	(−2.593)	(−1.631)	(1.968)	(13.653)	(6.69)	(1.873)	(−2.615)	(−3.839)	(−0.661)
					−0.219	0.173	−0.194					−0.141	−0.349	−0.445
					(−0.941)	(1.022)	(−0.526)					(−0.673)	(−1.473)	(−1.303)
RSV†		0.406	−0.216	0.382					0.238	0.103	0.235			
	0.169	(1.289)	(−0.619)	(0.719)				0.485	(4.129)	(1.032)	(2.205)			
	(2.048)	0.267	0.501	0.302				(10.05)	0.303	0.146	−0.109			
		(0.856)	(1.45)	(0.621)					(5.47)	(1.566)	(−0.98)			
RSVSJ†		−0.862	−0.883	−2.210	0.640	−2.097	0.582		0.268	0.229	0.218	−0.490	−1.969	−1.422
	0.421	(−1.544)	(−0.526)	(−0.830)	(0.634)	(−0.752)	(0.136)	1.009	(3.665)	(1.768)	(1.101)	(−1.413)	(−3.457)	(−1.124)
	(3.819)	1.633	1.512	3.027	−1.761	−1.75	−3.478	(5.733)	0.279	0.132	−0.063	−0.21	−0.648	−0.362
		(3.089)	(0.934)	(1.155)	(−2.949)	(−1.035)	(−1.254)		(3.848)	(1.163)	(−0.324)	(−0.698)	(−2.16)	(−0.594)
RSVSTJ†		−0.671	−3.545	−7.760	0.085	1.586	7.011		0.317	0.259	0.150	−0.689	−1.799	−0.710
	0.443	(−0.574)	(−1.207)	(−1.058)	(0.058)	(0.541)	(0.861)	0.949	(4.115)	(1.883)	(0.715)	(−2.241)	(−3.397)	(−0.689)
	(4.441)	1.511	4.076	8.361	−1.329	−3.779	−8.551	(6.580)	0.247	0.100	−0.044	−0.06	−0.152	−0.228
		(1.289)	(1.359)	(1.123)	(−1.044)	(−1.251)	(−1.109)		(3.271)	(0.84)	(−0.213)	(−0.258)	(−0.557)	(−0.385)

†: Results from positive (above) and Negative (below) estimators are separated by horizontal lines.

(A) BTC-D Coefficients and t-values of evolving. From Feb. 2017 to Feb. 2019

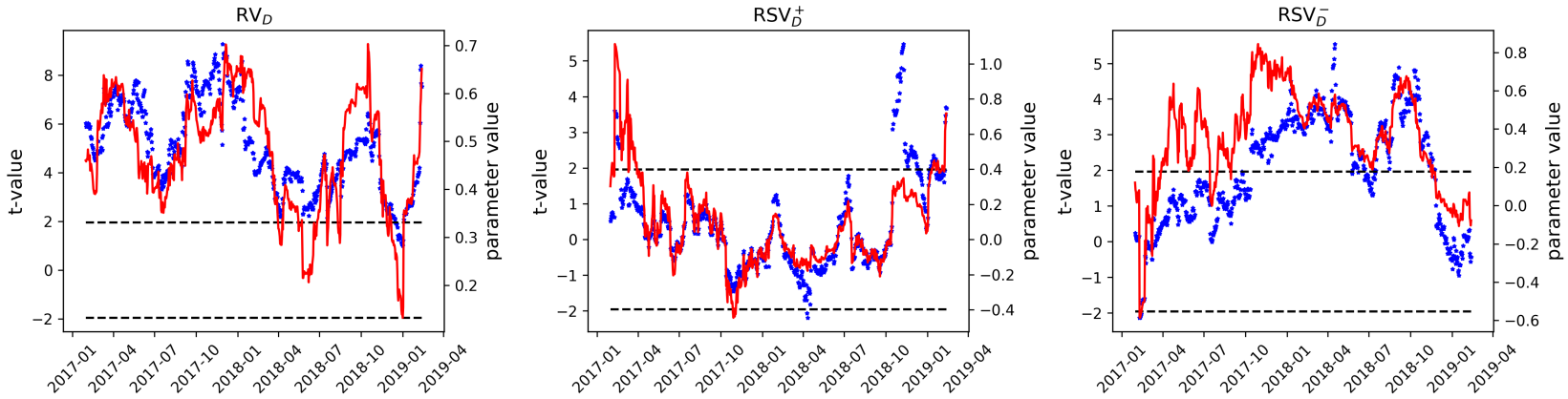

(B) BTC-G Coefficients and t-values of evolving. From Feb. 2017 to Apr. 2019

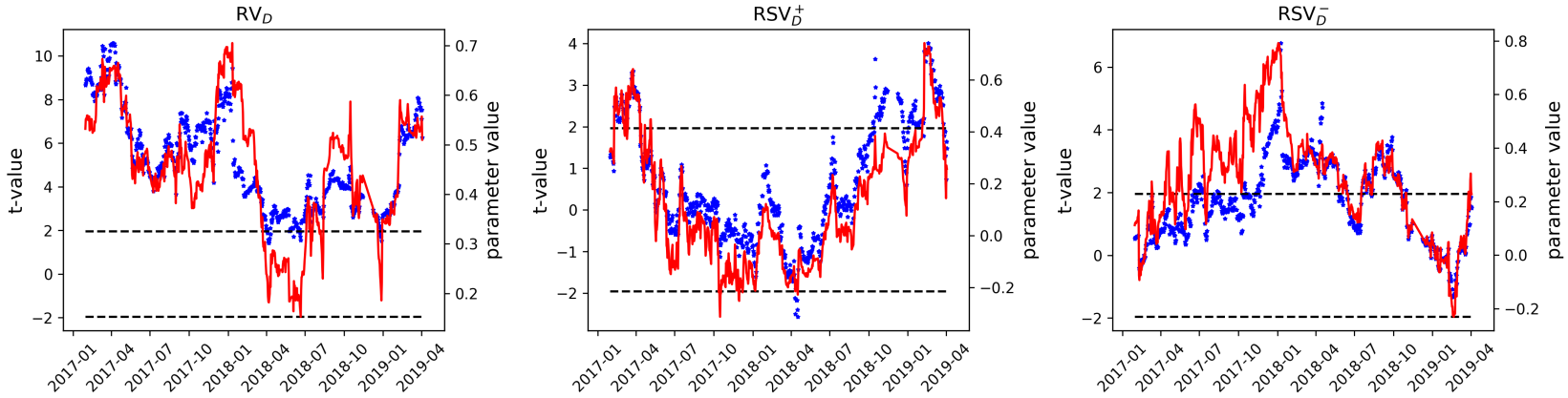

Figure 13: Parameter (in red line, left-axis) and its corresponding t-value (blue dots, right-axis) changes over time. For each panel, figures from left to right are coefficients of RV_D from HAR model, RSV_D^+ from HAR-RSV model, and RSV_D^- from HAR-RSV model, respectively. The dash line represents $t\text{-}value = \pm 1.987$. All models are in logarithmic form and horizon $h = 1$

RiskBTC_Plot

(A) BTC-D Coefficients and t-values of evolving. From Feb. 2017 to Feb. 2019

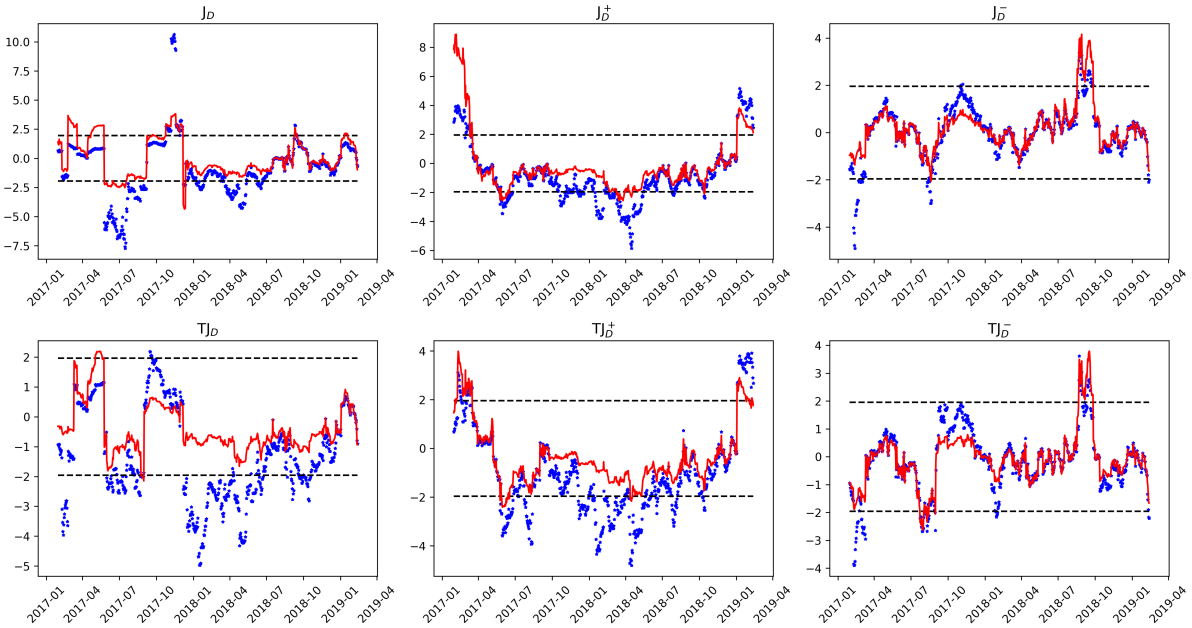

(B) BTC-G Coefficients and t-values of evolving. From Feb. 2017 to Apr. 2019

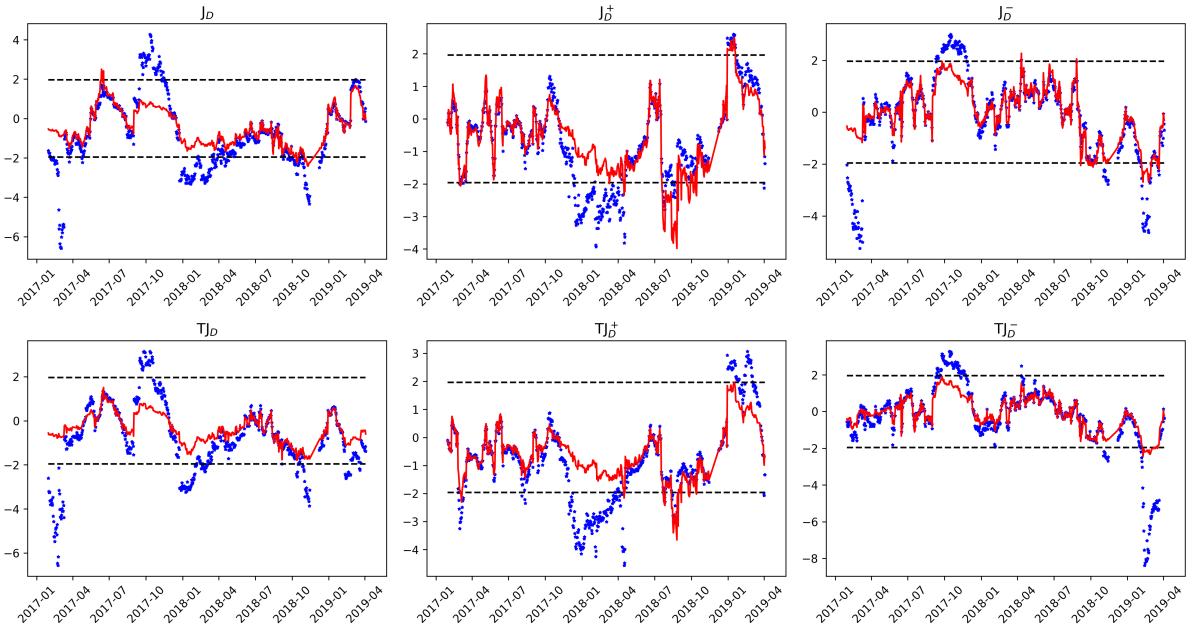

FIGURE 14: Parameter (in red line) and its corresponding t-value (blue dots) changes over time. For each panel, figures from (lower) upper left to (lower) upper right are coefficients of $(T)J_D$ from RV(T)J model, of $(T)J_D^+$ from RVS(T)J model, and $(T)J_D^-$ from RVS(T)J model, respectively. The dash line represents $t\text{-}value = \pm 1.987$. All models are in logarithmic form and horizon $h = 1$

RiskBTC_Plot

other hand, the upside risk RSV_D^+ tends to reduce market volatility during the same sample period, however, such an effect is not significant. Such finding is consistent with conclusion

in Patton and Sheppard (2015) which shows that RSV^- has stronger impact on future RV.

The downside risk is more informative than upside risk for those more volatile periods, in the meanwhile, positive jump $(T)J^+$ plays a quite significant role in reducing risk on the next day (Similar finding in Patton and Sheppard (2015)). Fig.14 compares the positive/negative jumps affect next day market risk. The positive jump coefficients β_{JD}^+ incline to be significant negative during those risky periods.

Noted that all results are drawn from models in logarithmic form, nevertheless, results from square form models show consistent results.

4.5. Out-of-Sample Forecasts Comparison

In this subsection, we further discuss the out-of-sample forecasting results aiming for comparing different models. All out-of-sample forecasts are computed using 90-days rolling-window HAR regressions as described in the previous sections. Parameters are re-estimated daily.

Negative forecasts occurred occasionally for square form models where the parameters have no restriction. Here the "insanity filter" is applied in which we ensure that any forecast is no smaller (larger) than the minimum (maximum) realization of the past (Patton and Sheppard (2015), Swanson and White (1997) and Bollerslev, Hood, Huss, and Pedersen (2018)).

All the out-of-sample performance evaluations are based on the square form, i.e RV. Results from the logarithmic form are transformed back to square form for a fair comparison. The comparison is based on the following metrics. First one is the adj-R^2 from Mincer-Zarnowitz regression, named MZ-R^2. The following three metrics named MSE, HRMSE, and QLIKE are computed from corresponding loss functions. And then the D-M test (Diebold and Mariano (2002)) is used to test the significance by embedding all the three loss functions.

$$\mathrm{L}^{\mathrm{MSE}} = \left(RV_{t,t+h} - \widehat{RV}_{t,t+h}\right)^2 \tag{21}$$

$$\mathrm{L}^{\mathrm{HRMSE}} = \left(\frac{RV_{t,t+h} - \widehat{RV}_{t,t+h}}{RV_{t,t+h}}\right)^2 \tag{22}$$

$$\mathrm{L}^{\mathrm{QLIKE}} = \log \widehat{RV}_{t,t+h} + \frac{RV_{t,t+h}}{\widehat{RV}_{t,t+h}} \tag{23}$$

The mean square error (MSE) is the mean value of quadratic loss function $\mathrm{L}^{\mathrm{MSE}}$ which measures the Euclidean distance between the ex-post realized variance RV and forecast

Table 6: Adaptive HAR Model Out-of-Sample Forecasts Performance Evaluation

	BTC-D								BTC-G							
	HAR	RVJ	RVTJ	RVSJ	RVSTJ	RSV	RSVSJ	RSVSTJ	HAR	RVJ	RVTJ	RVSJ	RVSTJ	RSV	RSVSJ	RSVSTJ
Square form																
		h=1														
MZ-R^2	0.267	0.227	0.248	0.228	0.219	0.285	0.215	0.165	0.213	0.179	0.182	0.182	0.190	0.226	0.144	0.151
MSE	3.636	4.023†	3.850	4.032	3.984	3.676	4.414†	4.812†	2.437	2.537	2.508	2.682	2.580	2.411	2.943	2.872
HRMSE	1.569	2.031†	1.576	1.792†	1.737†	1.767†	1.841†	1.756†	1.976	2.251†	2.080	2.497†	2.385†	2.022	2.762†	2.583†
QLIKE	0.846	1.151†	1.100†	1.000†	1.172†	0.988†	1.176†	1.545†	0.749	1.418†	1.636†	3.367†	2.406†	1.139†	3.548†	4.706†
		h=7														
MZ-R^2	0.365	0.360	0.416	0.440	0.470	0.431	0.508	0.458	0.355	0.349	0.360	0.420	0.425	0.424	0.481	0.435
MSE	1.643	1.789†	1.437	1.552	1.285*	1.573	1.328*	1.272*	0.990	0.905	0.888	0.889	0.830*	0.875*	0.812*	0.818*
HRMSE	1.359	1.646†	1.278	1.358	1.303	1.455	1.243	1.279	1.278	1.433†	1.366†	1.247	1.305	1.050*	1.232	1.624
QLIKE	0.984	1.146†	0.997	1.026	0.996	1.037	0.880*	1.043	0.797	1.152†	1.341†	1.818†	1.618†	0.878	1.679†	1.738†
		h=30														
MZ-R^2	0.543	0.583	0.682	0.717	0.623	0.628	0.743	0.677	0.635	0.667	0.682	0.702	0.693	0.707	0.791	0.813
MSE	0.673	0.649	0.462*	0.398*	0.558*	0.514*	0.357*	0.440*	0.314	0.261*	0.256*	0.243*	0.239*	0.235*	0.178*	0.147*
HRMSE	0.779	0.637*	0.614*	0.525*	0.528*	0.698*	0.483*	0.444*	0.696	0.611*	0.554*	0.490*	0.487*	0.529*	0.456*	0.404*
QLIKE	0.937	0.943	0.898*	0.847*	0.883*	0.877*	0.842*	0.874*	0.770	0.725*	0.743*	0.727*	0.754	0.722*	0.715*	0.741
Logarithmic form																
		h=1														
MZ-R^2	0.299	0.264	0.287	0.239	0.265	0.289	0.236	0.241	0.261	0.221	0.218	0.238	0.249	0.266	0.243	0.235
MSE	3.260	3.419†	3.356	3.657	3.501	3.313	3.773	3.680	2.217	2.329	2.353	2.284	2.260	2.209	2.262	2.298
HRMSE	0.760	0.893†	0.822†	0.963†	0.898†	0.807†	1.022†	0.937†	0.979	0.986	1.004	1.167	1.118	0.985	1.161	1.143
QLIKE	0.902	0.950	0.972	0.902	0.956	0.920	0.985	1.085†	0.906	0.998†	1.017	1.056†	1.074†	0.945	1.112†	1.170†
		h=7														
MZ-R^2	0.327	0.330	0.366	0.381	0.443	0.333	0.374	0.392	0.329	0.281	0.277	0.344	0.377	0.352	0.352	0.406
MSE	1.576	1.642	1.514	1.530	1.459	1.691	1.657	1.588	0.949	1.014	1.016	0.968	0.912	0.955	1.082	0.931
HRMSE	0.881	1.209	0.903	1.027	1.080	1.091†	0.986	0.969	0.908	0.906	0.989†	0.865	0.862	0.888	1.022	0.971
QLIKE	0.946	1.008†	0.947	0.917	0.904	0.946	0.907	0.930	0.906	0.909	1.001†	1.000	1.009†	0.929	0.945	0.978
		h=30														
MZ-R^2	0.504	0.549	0.680	0.604	0.591	0.569	0.639	0.604	0.591	0.626	0.635	0.651	0.671	0.632	0.678	0.708
MSE	0.729	0.681*	0.488*	0.531*	0.616*	0.611*	0.489*	0.584*	0.348	0.303*	0.305*	0.288*	0.276*	0.307*	0.267*	0.247*
HRMSE	0.628	0.493*	0.488*	0.691	0.654	0.543*	0.459*	0.451*	0.582	0.514*	0.549*	0.481*	0.461*	0.509*	0.397*	0.384*
QLIKE	0.965	0.936*	0.910*	0.900*	0.891*	0.885*	0.872*	0.878*	0.773	0.731*	0.746*	0.726*	0.736*	0.744*	0.715*	0.725*

All jumps are estimated under confidence level $\alpha = 99.99\%$.

†: Better forecasts from HAR model against of any other models by D-M test at 5% significant level.

∗: Worse forecasts from HAR model against of any other models by D-M test at 5% significant level.

result $\widehat{RV}$. The heteroskedasticity adjusted root mean square error (HRMSE) defined as the square root mean of $\mathrm{L}^{\mathrm{HRMSE}}$ (Bollerslev and Ghysels (1996)) is a more robust metric to the scale changing of realized variance. The third metric QLIKE is the mean of a gaussian quasi-likelihood loss function L^{QLIKE} (Patton (2011)) which gives consistent evaluation from different imperfect volatility proxies.

Out-of-sample forecasting evaluations reported in Tab.6 show consistently that the model performance comparison heavily relies on the choice of the forecasting horizon. First of all, it is obvious that most of the models perform better when they are in longer forecasting horizon setting, the MZ-R^2 are larger and the three metrics values are smaller. Those models that do not put jump components as explanatory variables separately, HAR and RSV models, tend to outperform any other models in short forecasting horizon cases. As shown by the D-M test evaluated at 5% significance level, forecasting errors generated by the HAR model are likely to be significantly smaller by the three loss functions when $h = 1$. However, the superiority of the HAR model vanishes as the forecasting horizon h increases. And when $h = 30$, HAR underperforms any other finer calibrated models.

4.6. Economic Value

The model performance is heavily influenced by the choice of metrics. An example being the upper-left panel of Tab.6 (square form, BTC-D when $h = 1$) which indicates that the HAR model performs worse than the RSV model by MZ-R^2, however, one can find that HAR has smaller forecasting errors than that of RSV by QLIKE.

As the validity of forecasting is to be tested by the market, we employ the approach of Bollerslev, Hood, Huss, and Pedersen (2018). Advantages of this approach relative to the framework of Fleming, Kirby, and Ostdiek (2001) are twofold. This so called RU-framework evaluates utility without requiring forecasts on asset returns. Then, it mimics a trading strategy when an investor targets at a constant Sharp ratio and adjust his/her risky asset positions according to the RV forecasts. A first order expansion on expected utility yields (for $h = 1$)

$$\mathrm{E}\left[u(W_{t+1})\right] = \mathrm{E}(W_{t+1}) - \frac{1}{2}\gamma^A \mathrm{V}(W_{t+1}), \tag{24}$$

where γ^A is the absolute Pratt-Arrow risk aversion.

The Realized Utility $RU_{t+1}^{(m)}$ at time $t+1$ by model m defined as utility per wealth with optimal weights $\mathrm{RU}_{t+1}^{(m)} = \mathrm{EU}(\omega_t^{(m)})/W_t$ is given by (More details refer to Appendix B.1):

$$\mathrm{RU}_{t+1}^{(m)} = \frac{SR^2}{\gamma}\left(\sqrt{\frac{RV_{t+1}}{\widehat{RV}_{t+1}^{(m)}}} - \frac{1}{2}\frac{RV_{t+1}}{\widehat{RV}_{t+1}^{(m)}}\right) \tag{25}$$

Following Bollerslev, Hood, Huss, and Pedersen (2018), here all results are based on Sharp ratio $SR = 0.4$ and relative risk aversion $\gamma = 2$. It is obvious that the $\mathrm{RU}_{t+1}^{(m)} = \frac{SR^2}{2\gamma} = 4\%$ if one has perfect forecast, i.e $\widehat{RV}_{t+1}^{(m)} = RV_{t+1}$.

Clearly, given SR/γ, lower risk the investor expects for the next day, a higher proportion of wealth should be allocated to risky asset. And in the case that $\sqrt{\widehat{RV}_{t+1}^{(m)}} < SR/\gamma$, then $\omega_t^{(m)} > 1$ which implies a leverage investment. However, we restrict the weight as $\omega_t \in [0, 1]$. Consequently, when $\omega_t^{(m)} > 1$, the realized utility $\mathrm{RU}_t^{(m)} = SR \cdot \sqrt{RV_{t+1}} - \frac{\gamma}{2} RV_{t+1}$.

$$\mathrm{RU}_t^{(m)} = \begin{cases} \frac{SR^2}{\gamma}\left(\sqrt{\frac{RV_{t+1}}{\widehat{RV}_{t+1}^{(m)}}} - \frac{1}{2}\frac{RV_{t+1}}{\widehat{RV}_{t+1}^{(m)}}\right), & \frac{SR}{\gamma} \leq \sqrt{\widehat{RV}_{t+1}^{(m)}} \\ SR \cdot \sqrt{RV_{t+1}} - \frac{\gamma}{2} RV_{t+1}, & \text{otherwise} \end{cases} \tag{26}$$

The realized utility $RU^{(m)}$ for each model m is averaging the $RU_t^{(m)}$ over time t.

$$RU^{(m)} = \frac{1}{T}\sum_{t=1}^{T} RU_t^{(m)} \tag{27}$$

Table 7: Economic Values Evaluation of Out-of-Sample Forecasts (%)

		HAR	RVJ	RVTJ	RVSJ	RVSTJ	RSV	RSVSJ	RSVSTJ
BTC-D	**Square form**								
	h=1	**2.938**	2.403	2.496	2.613	2.268	2.626	2.356	1.421
	h=7	3.071	2.614	3.048	2.935	3.024	2.916	**3.339**	2.874
	h=30	3.569	3.522	3.642	3.760	3.667	3.708	**3.769**	3.678
	Logarithmic form								
	h=1	**2.619**	2.486	2.404	2.660	2.486	2.583	2.403	2.146
	h=7	3.133	2.969	3.128	3.196	**3.234**	3.140	3.204	3.143
	h=30	3.479	3.527	3.591	3.619	3.641	3.671	**3.676**	3.665
BTC-G	**Square form**								
	h=1	**2.650**	1.364	1.330	−0.244	0.560	2.041	−0.421	−1.843
	h=7	**3.164**	2.271	1.862	0.569	1.294	2.906	1.090	1.100
	h=30	3.585	3.687	3.637	3.669	3.597	3.689	**3.697**	3.621
	Logarithmic form								
	h=1	**2.098**	1.871	1.728	1.663	1.584	2.019	1.513	1.393
	h=7	**2.793**	2.805	2.549	2.496	2.466	2.710	2.699	2.631
	h=30	3.576	3.668	3.633	3.672	3.647	3.635	**3.690**	3.662

All jumps are estimated under confidence level $\alpha = 99.99$. The highest utility number in each row is bolded.

The realized utility provides another metric to compare forecasts from different models. Clearly, the comparison almost solely depends on the forecasts $\widehat{RV}_{t+1}^{(m)}$ illustrated in (26).

And all evaluation results are shown in Tab.7. As explained above, better the forecast is, closer the $RU_{t+h}^{(m)}$ to 4%. Note that the RU_{t+h} metric could be negative as shown in Tab.7 where RSVSTJ model produces negative utility of -1.843 in the case of $h = 1$. Reason for that is severe under-forecasting on RV_{t+1}, i.e $RV_{t+1}/\widehat{RV}_{t+1}^{(m)} > 4$.

One investor can gain higher utility regardless of the choice of the model if one forecasts a longer horizon risk, e.g $h = 30$. For example, the HAR model gives around 63 basis points more utility in the case of $h = 30$ than that of $h = 1$. For short horizon risk forecasting, $h = 1$, the roughest model HAR, however, performs the best which outperforms the second-best model by up to 91 basis points. Modelling realized variance with the jump in short horizon risk forecasting case would not add economic values. On the other hand, for the longer horizon risk forecasting case, $h = 30$, accounting jump components does provide extra utility, e.g RSVSJ model outperforms HAR model by 20 basis points utility. Since the influence of separating jump components relies heavily on the forecasting horizon, given the investment horizon, investors who target at a certain risk level are required to select the forecasting model accordingly.

Last but not least, the investors can gain more utility by investing in BTC-D than on BTC-G in the short horizon risk forecasting case. BTC-D is a simple equal-weighted price portfolio which diversifies exchange idiosyncratic discontinuities changes risk (jumps) on price. While BTC-G suffers from the extra risk inherent in the one specific exchange.

5. Conclusion

This paper studies the risk of the Bitcoin market based on two high-frequency intraday data sources BTC-D and BTC-G for the sample period from January 2017 to Mid-2019.

First, we separate the risk sources of BTC in volatility and jumps employing the jump component separation method discussed in Barndorff-Nielsen and Shephard (2004) Barndorff-Nielsen and Shephard (2006) and Andersen, Bollerslev, and Diebold (2007). The BTC market is much riskier than any other developed financial markets in terms of realized variance and jumps. More than a quarter of the samples are identified as jump related.

However, we find that this separation method fails to display some of the obvious jumps on price process caused by consecutive jumps. The thresholded jump estimator TJ (Corsi, Pirino, and Reno (2010)) is further used to disentangle the jumps from RV. Empirically, TJ captures much more jumps by both size and quantity. Surprisingly, despite the jumps being detected frequently, the discontinuities do not contribute much to the risk compared with the continuous path. Our regression results latter show that TJ estimator reduces the market volatility on the next day more significant than J does.

Moreover, RV is further decomposed into positive estimators including upside risk RSV^+, positive jump $(T)J^+$, and negative estimators including downside risk RSV^-, negative jump $(T)J^-$ (Barndorff-Nielsen, Kinnebrock, and Shephard (2008), Patton and Sheppard (2015)). During our sample period, the number of positive jumps approximately equals to the number of negative jumps suggesting that jump is not a necessary crash event. Such finding is contrary to the empirical results in Scaillet, Treccani, and Trevisan (2018) concluding that most jumps in BTC are positive from June 2011 to November 2013. Note that the simple 3-exchange equal-weighted portfolio, BTC-D, can reduce the idiosyncratic jump risk significantly.

Then, 8 HAR-type models are developed to investigate how lagged $RV_{t-l,t}$, detected jumps $(T)J$ and signed estimators impact RV_{t+h}, $h = 1, 7, 30$. We first conduct a full in-sample regression and then proceed with a 90-day rolling window out-of-sample forecast in which parameters update daily. The in-sample evidence suggests that the higher downside risk RSV_D^- induces higher risk on the next day, while the higher positive jump $(T)J_D^+$ tends to reduce the risk on the next day. Those effects appear even more strongly during the volatile periods.

The comparison of out-of-sample forecasts between models heavily depends on the forecasting horizon h. For short-horizon forecasting, $h = 1$, both adding jump components to the basic HAR model and decomposing RV into RSV reduce forecasting accuracy surprisingly. This is likely caused by the overreaction on jumps from models. However, in the case of $h = 30$, the separation and decomposition models will outperform basic HAR model. The significance of the comparisons is confirmed by the D-M test. Then the forecasts are evaluated under the realized utility RU-framework (Bollerslev, Hood, Huss, and Pedersen (2018)) which mimics an investor who targets at constant Sharp ratio and rebalances the position according to the forecasts. Overall, an investor who forecasts longer horizon risk gains more utility than the one who forecasts over short-horizon risk no matter which model one selected. Significant result advocates that up to 20 basis points more utility can be obtained by calibrating finer models with signed estimators in the case of longer horizon forecast. Consistently, in a short-horizon forecast, modelling jumps do not provide extra utility. Last but not least, an investor who forecasts short-horizon can employ BTC-D to diversify idiosyncratic jump risk and gain higher utility.

Appendix A.

A.1. MPV

We start with the general definition of the MultiPower Variation MPV, for time period $[t, t+1]$:

$$MPV_{t+1}(\Delta, \eta_1, \ldots, \eta_m) \stackrel{\text{def}}{=} \left(\prod_{k=1}^{m} \mu_{\eta_k}^{-1} \right) \cdot \Delta^{1-\frac{1}{2}(\eta_1+\cdots+\eta_m)} \cdot \sum_{j=m}^{1/\Delta} \prod_{k=1}^{m} |r_{t+(j-k+1)\Delta}|^{\eta_k} \tag{28}$$

Where $\mu_{\eta_k} = 2^{\frac{\eta_k}{2}} \frac{\Gamma\{(\eta_k+1)/2\}}{\Gamma(\frac{1}{2})}$.

BPV in (5) is calculated by setting $m = 2$ and $\eta_1 = \eta_2 = 1$. And TPV is defined by setting $m = 3$ and $\eta_1 = \eta_2 = \eta_3 = 4/3$.

For given $\eta_k \geq 0, k = 1, 2, \ldots$ the convergence property is given by:

$$MPV_{t+1}(\Delta, \eta_1, \ldots, \eta_m) \xrightarrow{\text{p}} \int_t^{t+1} \sigma^{\eta_1+\cdots+\eta_m}(s) ds \tag{29}$$

A.2. TMPV

Thresholded MultiPower Variation $TMPV$ documented in Mancini (2009) is formulated as:

$$\begin{aligned} TMPV_{t+1}(\Delta, \eta_1, \ldots, \eta_m) = & \left(\prod_{k=1}^{m} \mu_{\eta_k}^{-1} \right) \cdot \Delta^{1-\frac{1}{2}(\eta_1+\cdots+\eta_m)} \\ & \cdot \sum_{j=m}^{1/\Delta} \prod_{k=1}^{m} |r_{t+(j-k+1)\Delta}|^{\eta_k} \\ & \cdot \mathbf{I}\left\{ |r_{t+(j-k+1)\Delta}|^2 \leq \theta_{t+(j-k+1)\Delta} \right\} \end{aligned} \tag{30}$$

A.3. Local Variance Estimation

We employ the nonparametric local variance estimate Fan and Yao (2008)

$$\widehat{V}_t^{[n]} = \frac{\sum_{i=-l, i\neq -1,0,1}^{l} K(\frac{i}{l}) \cdot r_{t+i}^2 \cdot \mathbf{I}\{r_{t+i}^2 \leq c_\theta^2 \cdot \widehat{V}_{t+i}^{[n-1]}\}}{\sum_{i=-l, i\neq -1,0,1}^{l} K(\frac{i}{l}) \cdot \mathbf{I}\{r_{t+i}^2 \leq c_\theta^2 \cdot \widehat{V}_{t+i}^{[n-1]}\}}, n = 1, 2, 3... \tag{31}$$

Where K is a Gaussian kernel with bandwidth value $l = 25$. To avoid using future information and for computational simplicity, $\widehat{V}_t$ is estimated within each day. Thus, the

first and last l-points of $\widehat{V}_t$ each day are smoothed by only partial Gaussian kernel. This recursive computation stops when the change from last step is smaller than a given criterion.

A.4. Conditional Expected Return

The expected value of η-power returns conditioning on the square returns larger than threshold

$$\begin{aligned} r^e(\theta,\eta) &= \mathrm{E}\left\{ |r|^\eta \middle| r^2 > \theta \right\} \\ &= \frac{(2\sigma^2)^{\frac{\eta}{2}}}{2\sqrt{\pi}\Phi\left(-\frac{\sqrt{\theta}}{\sigma}\right)} \cdot \Gamma\left(\frac{\eta+1}{2}, \frac{\theta}{2\sigma^2}\right) \end{aligned} \tag{32}$$

Given that the σ^2 is approximated by $\widehat{V}_t$, we have:

$$r^e(\theta_t,\eta) = \frac{1}{2\sqrt{\pi}\Phi\left(-c_\theta\right)} \cdot \left(\frac{2\theta_t}{c_\theta^2}\right)^{\frac{\eta}{2}} \cdot \Gamma\left(\frac{\eta+1}{2}, \frac{c_\theta^2}{2}\right) \tag{33}$$

Where $\Phi(x)$ is cdf of N(0,1) and $\Gamma(\alpha,x) = \int_x^{+\infty} s^{\alpha-1}e^{-s}ds$ is the upper incomplete gamma function.

A.5. Corrected TMPV

The Corrected version of $TMPV$ is defined as:

$$TMPV_{t+1}(\Delta,\eta_1,\ldots,\eta_m) \overset{\text{def}}{=} \left(\prod_{k=1}^{m}\mu_{\eta_k}^{-1}\right)\cdot\Delta^{1-\frac{1}{2}(\eta_1+\cdots+\eta_m)}\cdot\sum_{j=m}^{1/\Delta}\prod_{k=1}^{m} C_{\eta_k}\left(r_{t+(j-k+1)\Delta},\theta_{t+(j-k+1)\Delta}\right) \tag{34}$$

We specify $m=2,\eta_1=\eta_2=1$ for $TBPV$, and $m=3,\eta_1=\eta_2=\eta_3=\frac{4}{3}$ for estimating $TTPV$.

A.6. Jump Test z-test

Based on the distribution results from Barndorff-Nielsen and Shephard (2004) and other extensions in which the statistic goes to normal distribution given a series of conditions and in the absence of jump. The z-test is the ratio-statistic provided by Huang and Tauchen (2005).

$$z_{t+1} = \frac{\{RV_{t+1}(\Delta) - BPV_{t+1}(\Delta)\} RV_{t+1}^{-1}(\Delta)}{\sqrt{\Delta \cdot \zeta \cdot \max\left\{1, \frac{TPV_{t+1}(\Delta)}{\{BPV_{t+1}(\Delta)\}^2}\right\}}} \tag{35}$$

Where $\zeta = \frac{\pi^2}{4} + \pi - 5$,

Appendix B.

B.1. Realized Utility

A first order expansion on expected utility yields (for $h = 1$)

$$\mathrm{E}\left[u(W_{t+1})\right] = \mathrm{E}(W_{t+1}) - \frac{1}{2}\gamma^A \mathrm{V}(W_{t+1}), \tag{36}$$

where γ^A is the absolute Pratt-Arrow risk aversion. The wealth function W is explicitly given by (37) for allocating ω_t proportion of whole wealth on the risky asset, and $r_{t+1} - r_f$ is the unknown excess return.

$$\begin{aligned} W_{t+1} &= W_t\{1 + (1 - \omega_t)r_f + \omega_t r_{t+1}\} \\ &= W_t\{1 + r_f + \omega_t(r_{t+1} - r_f)\} \end{aligned} \tag{37}$$

Assuming that the risk-free interest rate r_f is constant, W_t and ω_t are known, the expect value and variance of W_{t+1} is:

$$\begin{aligned} \mathrm{E}(W_{t+1}) &= W_t(1 + r_f) + W_t\omega_t\,(\,r_{t+1} - r_f) \\ \mathrm{V}(W_{t+1}) &= W_t^2\omega_t^2 \cdot \mathrm{V}(r_{t+1} - r_f) \end{aligned} \tag{38}$$

Given a target Sharp ratio $SR = \frac{\mathrm{E}(r_{t+1})}{\sqrt{\mathrm{V}(r_{t+1})}}$, (38) and (36) give the following expression of expected utility $EU(\omega_t)$ $\mathrm{EU}(\omega_t)$ with replacing $\mathrm{V}(r_{t+1})$ by RV_{t+1}

$$\begin{aligned} \mathrm{EU}(\omega_t) &= W_t\left[\omega_t\,\mathrm{E}(r_{t+1}) - \frac{\gamma}{2}\omega_t^2\,\mathrm{V}(r_{t+1})\right] \\ &= W_t\left[\omega_t\,\mathrm{E}(r_{t+1}) - \frac{\gamma}{2}\omega_t^2 RV_{t+1}\right] \\ &= W_t\left[\omega_t \cdot SR \cdot \sqrt{RV_{t+1}} - \frac{\gamma}{2}\omega_t^2 RV_{t+1}\right] \end{aligned} \tag{39}$$

Here the $\gamma = \gamma^A W_t$ represents the relative risk aversion. Based on the out-of-sample forecasts $\widehat{RV}_{t+1}^{(m)}$ from model m, one can derive the optimal weight $\omega_t^{(m)}$ targeting SR/γ.

$$\omega_t^{(m)} = \frac{SR/\gamma}{\sqrt{\widehat{RV}_{t+1}^{(m)}}} \tag{40}$$

The Realized Utility $RU_{t+1}^{(m)}$ at time $t+1$ by model m defined as utility per wealth with optimal weights $\mathrm{RU}_{t+1}^{(m)} = \mathrm{EU}(\omega_t^{(m)})/W_t$ can be obtained by (40) and (39).

$$\mathrm{RU}_{t+1}^{(m)} = \frac{SR^2}{\gamma}\left(\sqrt{\frac{RV_{t+1}}{\widehat{RV}_{t+1}^{(m)}}} - \frac{1}{2}\frac{RV_{t+1}}{\widehat{RV}_{t+1}^{(m)}}\right) \tag{41}$$

References

Ait-Sahalia, Y., P. A. Mykland, and L. Zhang (2005): "How Often to Sample a Continuous-time Process in the Presence of Market Microstructure Noise," *The Review of Financial Studies*, 18(2), 351–416.

Andersen, T. G., T. Bollerslev, and F. X. Diebold (2007): "Roughing It up: Including Jump Components in the Measurement, Modeling, and Forecasting of Return Volatility," *The Review of Economics and Statistics*, 89(4), 701–720.

Andersen, T. G., T. Bollerslev, F. X. Diebold, and H. Ebens (2001): "The Distribution of Realized Stock Return Volatility," *Journal of Financial Economics*, 61(1), 43–76.

Andersen, T. G., T. Bollerslev, F. X. Diebold, and P. Labys (2001): "The Distribution of Realized Exchange Rate Volatility," *Journal of the American Statistical Association*, 96(453), 42–55.

Balcilar, M., E. Bouri, R. Gupta, and D. Roubaud (2017): "Can Volume Predict Bitcoin Returns and Volatility? a Quantiles-based Approach," *Economic Modelling*, 64, 74–81.

Bandi, F. M., and J. R. Russell (2008): "Microstructure Noise, Realized Variance, and Optimal Sampling," *Review of Economic Studies*, 75(2), 339–369.

Barndorff-Nielsen, O. E., P. R. Hansen, A. Lunde, and N. Shephard (2008): "Designing realized kernels to measure the ex post variation of equity prices in the presence of noise," *Econometrica*, 76(6), 1481–1536.

Barndorff-Nielsen, O. E., S. Kinnebrock, and N. Shephard (2008): "Measuring Downside Risk-realised Semivariance," *CREATES Research Paper*, (2008-42).

Barndorff-Nielsen, O. E., and N. Shephard (2002a): "Econometric Analysis of Realized Volatility and Its Use in Estimating Stochastic Volatility Models," *Journal of the Royal Statistical Society: Series B (Statistical Methodology)*, 64(2), 253–280.

——— (2002b): "Estimating Quadratic Variation Using Realized Variance," *Journal of Applied Econometrics*, 17(5), 457–477.

——— (2004): "Power and Bipower Variation with Stochastic Volatility and Jumps," *Journal of Financial Econometrics*, 2(1), 1–37.

——— (2006): "Econometrics of Testing for Jumps in Financial Economics Using Bipower Variation," *Journal of Financial Econometrics*, 4(1), 1–30.

Bollerslev, T., and E. Ghysels (1996): "Periodic Autoregressive Conditional Heteroscedasticity," *Journal of Business & Economic Statistics*, 14(2), 139–151.

Bollerslev, T., B. Hood, J. Huss, and L. H. Pedersen (2018): "Risk Everywhere: Modeling and Managing Volatility," *The Review of Financial Studies*, 31(7), 2729–2773.

Bouri, E., P. Molnár, G. Azzi, D. Roubaud, and L. I. Hagfors (2017): "On the Hedge and Safe Haven Properties of Bitcoin: Is It Really More Than a Diversifier?," *Finance Research Letters*, 20, 192–198.

Bukovina, J., M. Martičekˇ, et al. (2016): "Sentiment and Bitcoin Volatility," Discussion paper, Mendel University in Brno, Faculty of Business and Economics.

Chen, S., C. Y.-H. Chen, W. K. Härdle, T. Lee, and B. Ong (2018): "Econometric Analysis of a Cryptocurrency Index for Portfolio Investment," in *Handbook of Blockchain, Digital Finance, and Inclusion, Volume 1*, pp. 175–206. Elsevier.

Conrad, C., A. Custovic, and E. Ghysels (2018): "Long-and Short-Term Cryptocurrency Volatility Components: A GARCH-MIDAS Analysis," *Journal of Risk and Financial Management*, 11(2), 23.

Corsi, F. (2009): "A Simple Approximate Long-memory Model of Realized Volatility," *Journal of Financial Econometrics*, 7(2), 174–196.

Corsi, F., D. Pirino, and R. Reno (2010): "Threshold Bipower Variation and the Impact of Jumps on Volatility Forecasting," *Journal of Econometrics*, 159(2), 276–288.

Diebold, F. X., and R. S. Mariano (2002): "Comparing Predictive Accuracy," *Journal of Business & Economic Statistics*, 20(1), 134–144.

Dyhrberg, A. H. (2016): "Bitcoin, Gold and the Dollar – a GARCH Volatility Analysis," *Finance Research Letters*, 16, 85–92.

Fan, J., and Q. Yao (2008): *Nonlinear Time Series: Nonparametric and Parametric Methods*. Springer Science & Business Media.

Fleming, J., C. Kirby, and B. Ostdiek (2001): "The Economic Value of Volatility Timing," *The Journal of Finance*, 56(1), 329–352.

Garcia, D., and F. Schweitzer (2015): "Social Signals and Algorithmic Trading of Bitcoin," *Royal Society open science*, 2(9), 150288.

Gerlach, J.-C., G. Demos, and D. Sornette (2019): "Dissection of Bitcoin's multiscale bubble history from January 2012 to February 2018," *Royal Society Open Science*, 6(7), 180643.

Glaser, F., K. Zimmermann, M. Haferkorn, M. C. Weber, and M. Siering (2014): "Bitcoin-asset or Currency? Revealing Users' Hidden Intentions," *Revealing Users' Hidden Intentions (April 15, 2014). ECIS*.

Griffin, J. M., and A. Shams (2018): "Is Bitcoin Really Un-Tethered?," *Avaiable at SSRN: https://ssrn.com/abstract=3195066*.

Gronwald, M. (2014): "The Economics of Bitcoins–Market Characteristics and Price Jumps," *Available at SSRN: https://ssrn.com/abstract=2548999*.

Hafner, C. M. (2018): "Testing for Bubbles in Cryptocurrencies with Time-Varying Volatility," *Journal of Financial Econometrics*.

Hansen, P. R., and A. Lunde (2006): "Realized Variance and Market Microstructure Noise," *Journal of Business & Economic Statistics*, 24(2), 127–161.

Hou, A. J., W. Wang, C. Y. Chen, and W. K. Härdle (2018): "Pricing Cryptocurrency Options: The Case of Bitcoin and CRIX," *Available at SSRN: https://ssrn.com/abstract=3159130*.

Huang, X., and G. Tauchen (2005): "The Relative Contribution of Jumps to Total Price Variance," *Journal of Financial Econometrics*, 3(4), 456–499.

Liu, L. Y., A. J. Patton, and K. Sheppard (2015): "Does anything beat 5-minute RV? A comparison of realized measures across multiple asset classes," *Journal of Econometrics*, 187(1), 293–311.

Mancini, C. (2009): "Non-parametric Threshold Estimation for Models with Stochastic Diffusion Coefficient and Jumps," *Scandinavian Journal of Statistics*, 36(2), 270–296.

Mancini, C., and R. Renò (2011): "Threshold Estimation of Markov Models with Jumps and Interest Rate Modeling," *Journal of Econometrics*, 160(1), 77–92.

Nakamoto, S. (2008): "Bitcoin: A Peer-to-peer Electronic Cash System," .

Patton, A. J. (2011): "Volatility Forecast Comparison Using Imperfect Volatility Proxies," *Journal of Econometrics*, 160(1), 246–256.

Patton, A. J., and K. Sheppard (2015): "Good volatility, bad volatility: Signed jumps and the persistence of volatility," *Review of Economics and Statistics*, 97(3), 683–697.

Pichl, L., and T. Kaizoji (2017): "Volatility Analysis of Bitcoin Price Time Series," *Quantitative Finance and Economics*, 1, 474–485.

Scaillet, O., A. Treccani, and C. Trevisan (2018): "High-Frequency Jump Analysis of the Bitcoin Market*," *Journal of Financial Econometrics*.

Swanson, N. R., and H. White (1997): "Forecasting Economic Time Series Using Flexible Versus Fixed Specification and Linear Versus Nonlinear Econometric Models," *International Journal of Forecasting*, 13(4), 439–461.

Traian Pele, D., W. Niels, W. K. Härdle, M. Kolossiatis, and Y. Yatracos (2019): "Phenotypic convergence of cryptocurrencies," *IRTG 1792 Discussion Paper*.

Trimborn, S., and W. K. Härdle (2018): "CRIX an Index for Cryptocurrencies," *Journal of Empirical Finance*, 49, 107–122.

Urquhart, A., and H. Zhang (2019): "Is Bitcoin a Hedge or Safe Haven for Currencies? an Intraday Analysis," *International Review of Financial Analysis*, 63, 49–57.

Yermack, D. (2015): "Is Bitcoin a Real Currency? an Economic Appraisal," in *Handbook of digital currency*, pp. 31–43. Elsevier.

Zhang, L. (2006): "Efficient Estimation of Stochastic Volatility Using Noisy Observations: A Multi-scale Approach," *Bernoulli*, 12(6), 1019–1043.

Zhang, L., P. A. Mykland, and Y. Aït-Sahalia (2005): "A Tale of Two Time Scales," *Journal of the American Statistical Association*, 100(472), 1394–1411.

IRTG 1792 Discussion Paper Series 2019

For a complete list of Discussion Papers published, please visit http://irtg1792.hu-berlin.de.

001 "Cooling Measures and Housing Wealth: Evidence from Singapore" by Wolfgang Karl Härdle, Rainer Schulz, Taojun Xie, January 2019.

002 "Information Arrival, News Sentiment, Volatilities and Jumps of Intraday Returns" by Ya Qian, Jun Tu, Wolfgang Karl Härdle, January 2019.

003 "Estimating low sampling frequency risk measure by high-frequency data" by Niels Wesselhöfft, Wolfgang K. Härdle, January 2019.

004 "Constrained Kelly portfolios under alpha-stable laws" by Niels Wesselhöfft, Wolfgang K. Härdle, January 2019.

005 "Usage Continuance in Software-as-a-Service" by Elias Baumann, Jana Kern, Stefan Lessmann, February 2019.

006 "Adaptive Nonparametric Community Detection" by Larisa Adamyan, Kirill Efimov, Vladimir Spokoiny, February 2019.

007 "Localizing Multivariate CAViaR" by Yegor Klochkov, Wolfgang K. Härdle, Xiu Xu, March 2019.

008 "Forex Exchange Rate Forecasting Using Deep Recurrent Neural Networks" by Alexander J. Dautel, Wolfgang K. Härdle, Stefan Lessmann, Hsin-Vonn Seow, March 2019.

009 "Dynamic Network Perspective of Cryptocurrencies" by Li Guo, Yubo Tao, Wolfgang K. Härdle, April 2019.

010 "Understanding the Role of Housing in Inequality and Social Mobility" by Yang Tang, Xinwen Ni, April 2019.

011 "The role of medical expenses in the saving decision of elderly: a life cycle model" by Xinwen Ni, April 2019.

012 "Voting for Health Insurance Policy: the U.S. versus Europe" by Xinwen Ni, April 2019.

013 "Inference of Break-Points in High-Dimensional Time Series" by Likai Chen, Weining Wang, Wei Biao Wu, May 2019.

014 "Forecasting in Blockchain-based Local Energy Markets" by Michael Kostmann, Wolfgang K. Härdle, June 2019.

015 "Media-expressed tone, Option Characteristics, and Stock Return Predictability" by Cathy Yi-Hsuan Chen, Matthias R. Fengler, Wolfgang K. Härdle, Yanchu Liu, June 2019.

016 "What makes cryptocurrencies special? Investor sentiment and return predictability during the bubble" by Cathy Yi-Hsuan Chen, Roméo Després, Li Guo, Thomas Renault, June 2019.

017 "Portmanteau Test and Simultaneous Inference for Serial Covariances" by Han Xiao, Wei Biao Wu, July 2019.

018 "Phenotypic convergence of cryptocurrencies" by Daniel Traian Pele, Niels Wesselhöfft, Wolfgang K. Härdle, Michalis Kolossiatis, Yannis Yatracos, July 2019.

019 "Modelling Systemic Risk Using Neural Network Quantile Regression" by Georg Keilbar, Weining Wang, July 2019.

IRTG 1792, Spandauer Strasse 1, D-10178 Berlin
http://irtg1792.hu-berlin.de

This research was supported by the Deutsche Forschungsgemeinschaft through the IRTG 1792.

IRTG 1792 Discussion Paper Series 2019

For a complete list of Discussion Papers published, please visit http://irtg1792.hu-berlin.de.

020 "Rise of the Machines? Intraday High-Frequency Trading Patterns of Cryptocurrencies" by Alla A. Petukhina, Raphael C. G. Reule, Wolfgang Karl Härdle, July 2019.

021 "FRM Financial Risk Meter" by Andrija Mihoci, Michael Althof, Cathy Yi-Hsuan Chen, Wolfgang Karl Härdle, July 2019.

022 "A Machine Learning Approach Towards Startup Success Prediction" by Cemre Ünal, Ioana Ceasu, September 2019.

023 "Can Deep Learning Predict Risky Retail Investors? A Case Study in Financial Risk Behavior Forecasting" by A. Kolesnikova, Y. Yang, S. Lessmann, T. Ma, M.-C. Sung, J.E.V. Johnson, September 2019.

024 "Risk of Bitcoin Market: Volatility, Jumps, and Forecasts" by Junjie Hu, Weiyu Kuo, Wolfgang Karl Härdle, October 2019.

IRTG 1792, Spandauer Strasse 1, D-10178 Berlin
http://irtg1792.hu-berlin.de

This research was supported by the Deutsche Forschungsgemeinschaft through the IRTG 1792.